RESEARCH ARTICLE

Title: Sulfur oxidation and reduction are coupled to nitrogen fixation in the roots of a salt marsh foundation plant species

Authors: Rolando, J.L.[a]; Kolton, M.[a,b]; Song, T.[a], Liu, Y.[a,c]; Pinamang, P.[a], Conrad, R.[a]; Morris, J.T.[d], Konstantinidis, K.T.[a,e], Kostka, J.E. [a,f,g]

Affiliations:

[a]Georgia Institute of Technology, School of Biological Sciences, Atlanta, GA 30332, USA

[b]French Associates Institute for Agriculture and Biotechnology of Drylands, Ben-Gurion University of the Negev, Beer Sheva, Israel

[c]The Pennsylvania State University, Department of Civil & Environmental Engineering, University Park, PA, 16802

[d] Belle Baruch Institute for Marine & Coastal Sciences, University of South Carolina, Columbia, SC, 29201

[e]Georgia Institute of Technology, School of Civil and Environmental Engineering, Atlanta, GA 30332, USA

[f]Georgia Institute of Technology, School of Earth and Atmospheric Sciences, Atlanta, GA 30332, USA

[g]Center for Microbial Dynamics and Infection, Georgia Institute of Technology, Atlanta, GA 30332, USA

Corresponding author:

Kostka, JE. e-mail: joel.kostka@biology.gatech.edu

Abstract

Symbiotic root microbiota are crucial for plant growth as they assist their hosts in nutrient acquisition. In the roots of coastal marine plants, heterotrophic activity in the rhizosphere by sulfate-reducing microorganisms has been linked to nitrogen fixation. In this study, we recovered 239 high-quality metagenome-assembled genomes (MAGs) from a salt marsh dominated by the foundation plant *Spartina alterniflora*, including diazotrophic sulfate-reducing and sulfur-oxidizing bacteria thriving in the root compartment. Here we show for the first time that highly-abundant sulfur-oxidizing bacteria in the roots of a coastal macrophyte encode and highly express genes for nitrogen fixation (nifHDK). Further, we leveraged a *S. alterniflora* biomass gradient to gain a mechanistic understanding on how root-microbe interactions respond to abiotic stress from anoxia and elevated sulfide concentration. We observed that the roots of the stressed *S. alterniflora* phenotype exhibited the highest rates of nitrogen fixation and expression levels of both the oxidative and reductive forms of the dissimilatory sulfite reductase gene (dsrAB). Approximately 25% and 15% of all sulfur-oxidizing dsrA and nitrogen-fixing nifK transcripts, respectively, were associated with novel MAGs of the *Candidatus* Thiodiazotropha genus in the roots of the stressed *S. alterniflora* phenotype. We conclude that the rapid cycling of sulfur in the dynamic *S. alterniflora* root zone is coupled to nitrogen fixation during both reductive and oxidative sulfur reactions, and that the *S. alterniflora – Ca.* Thiodiazotropha symbiosis is an adaptive response to anoxic and sulfidic sediment conditions, whereby the plants benefit from reduced sulfide toxicity and potential nitrogen acquisition.

Introduction

The microbial communities closely associated with plant hosts (i.e., plant microbiota) have received substantial attention due to their potential role in plant nutrient acquisition, phytohormone synthesis, prevention of soil-borne disease, and detoxification of the rhizosphere and root environment (Bulgarelli et al., 2013; Trivedi et al., 2020). Most plant microbiome studies have been performed in terrestrial ecosystems with an emphasis on agricultural plants (Trivedi et al., 2020). Plant microbiota from vegetated coastal ecosystems (i.e., seagrass meadows, mangroves, and salt marshes) remain mostly understudied, even though they play a key role in global climate regulation and the cycling of major nutrients (Barbier et al., 2011; Duarte et al., 2013). Covering less than 3% of the global surface area occupied by forests, coastal vegetated ecosystems exhibit an equivalent rate of carbon sequestration at the planetary scale due to their excess in primary production over organic matter decomposition (Duarte et al., 2013). Further, vegetated estuarine ecosystems play a key role in water purification by reducing coastal nutrient pollution (Barbier et al., 2011). Despite their high ecological value, little is known about how plant-microbe interactions contribute to the functioning of coastal marine ecosystems, their resilience to climate change, and provisioning of ecosystem services.

Previous studies have shown that the root zone of coastal marine plants is a hotspot for the cycling of carbon, nitrogen, and sulfur (Gandy and Yoch, 1988; Welsh et al., 1996; Spivak and Reeve, 2015; Thomas et al., 2014; Crump et al., 2018; Kolton et al., 2020). In coastal Georgia, US, sulfate-reducing and sulfur-oxidizing bacteria were recently shown to be overrepresented in the core root microbiome of the salt marsh foundation plant *Spartina alterniflora*, comprised of persistent taxa across multiple plant individuals (Rolando et al., 2022). Sulfate reduction, an anaerobic respiration pathway, represents a dominant terminal electron-accepting process coupled to the breakdown of

68 organic matter in marine ecosystems (Kostka et al., 2002; Jørgensen et al., 2019). Evidence from
69 experimental and field research indicates that rhizospheric sulfate-reducing bacteria assimilate
70 photosynthates from *S. alterniflora*, while fueling nitrogen fixation (Gandy and Yoch, 1988;
71 Spivak and Reeve, 2015). Similarly, rates of nitrogen fixation have been closely associated with
72 organic matter degradation by sulfate reduction in seagrass meadows (McGlathery et al., 1998;
73 Herbert, 1999; Nielsen et al., 2001; Welsh et al., 1996). Conversely, the oxidation of reduced sulfur
74 compounds is a chemolithotrophic process requiring potent terminal electron acceptors such as
75 oxygen, nitrate, or oxidized metals. In particular, sulfide is a known phytotoxin, and its
76 belowground oxidation is considered a detoxifying reaction for plants inhabiting coastal marine
77 ecosystems (Lamers et al., 2013). Based on amplicon sequencing of the 16S rRNA gene, sulfur
78 oxidation coupled with nitrogen fixation was recently hypothesized as an important process for
79 plant growth under sulfidic conditions (Rolando et al., 2022). Nitrogen is often the limiting nutrient
80 for salt marsh plants, and stress from sulfide toxicity and anoxia further impairs root active
81 acquisition of nitrogen (Mendelssohn and Morris, 2000). Close relatives of diazotrophic sulfur-
82 oxidizing symbionts from the *Sedimenticolaceae* family (genus: *Candidatus* Thiodiazotropha)
83 have been shown to inhabit the roots of seagrasses and marsh plants in coastal marine ecosystems
84 (Martin et al., 2020a, Rolando et al., 2022). The *Ca.* Thiodiazotropha genus was first discovered
85 as bacterial symbionts of lucinid clams, where they provide both fixed carbon and nitrogen to their
86 animal host by sulfur-mediated chemolithoautotrophy (Petersen et al., 2017). Most studies
87 assessing the ecology and function of sulfur chemosymbiosis have been performed within marine
88 invertebrates hosts (Petersen et al., 2017; Osvatic et al., 2021, 2023; Lim et al., 2019a, 2019b). In
89 contrast, there is still no evidence for the coupling of sulfur oxidation with nitrogen and/or carbon
90 fixation in the roots of coastal marine plants because the genomes, metabolic potential, and activity

91 of root-associated sulfur-oxidizing bacteria are still lacking. Limited studies have looked into the
92 composition and abundance of sulfur-oxidizing bacteria present in the roots of coastal marine
93 plants. These studies mainly relied on microscopy- and DNA/RNA amplicon-based community
94 analyses (Thomas et al., 2014; Martin et al., 2020a; Kolton et al., 2020; Rolando et al., 2022). Only
95 one study utilized a metatranscriptomics approach to investigate the gene expression of seagrass
96 root-associated microbiomes (Crump et al., 2018). However, genome-wide gene expression
97 profiles of sulfur-oxidizing bacteria and the coupling of sulfur oxidation with other
98 biogeochemical processes are still to be deciphered in the roots of coastal marine plants.

99 Ecosystem models and empirical evidence indicate that climate change is altering the hydrology,
100 biogeochemistry, and plant community composition of coastal wetlands (Guimond et al., et al.,
101 2020; Donnelly and Bertness, 2001). Thus, a mechanistic understanding of how environmental
102 perturbations impact plant-microbe interactions will be critical to forecasting the resilience of salt
103 marsh ecosystems to climate change. According to the stress-gradient hypothesis (SGH), the
104 frequencies of facilitative and competitive interactions are inversely related along abiotic stress
105 gradients, with facilitative interactions occurring more frequently under high abiotic stress than
106 under benign conditions (Bertness and Callaway, 1994). This concept has mostly been explored in
107 plant-plant interactions; whereas, limited studies assessing plant-microbe interactions have found
108 that the SGH is consistent in certain plant phenological stages (David et al., 2020). Following the
109 SGH, we hypothesize that beneficial plant-microbe interactions will be more common in stressed
110 coastal marine ecosystems, where plants experience greater salinity, redox, and sulfide toxicity
111 stress. *S. alterniflora*-dominated salt marsh ecosystems represent an ideal natural laboratory in
112 which to study the effects of stress on plant-microbe interactions because steep gradients in plant
113 productivity are formed within short distances (Mendelssohn and Morris, 2000). The productivity

114 gradient is the result of decreased soil redox potential, along with increased salinity and anoxia,
115 extending from vegetated tidal creek banks towards the interior of the marsh (Figure 1). Higher
116 primary productivity is reflected in tall *S. alterniflora* plants (> 80 cm) growing adjacent to tidal
117 creek banks, while smaller plants (< 50 cm) inhabit the interior of the marsh. We hypothesize that
118 the strength of plant-sulfur chemosymbiosis increases in stressed marshes where elevated sulfide
119 oxidation rates are coupled to nitrogen fixation.

120 Thus, the objectives of the present study were: (i.), to demonstrate the coupling of sulfur oxidation
121 with nitrogen fixation in the root environment of *S. alterniflora* and (ii.) to evaluate the effect of
122 environmental stress on the assembly, activity, and ecological interactions of the *S. alterniflora*
123 root microbiome.

124 **2. Results**

125 <u>2.1 Genome-centric multi-omics approach reveals prokaryotic sulfur metabolism is coupled to</u>
126 <u>nitrogen fixation in the roots of a foundation salt marsh plant</u>

127 We studied the root microbiome of the salt marsh foundation species of the US Atlantic and Gulf
128 of Mexico coastlines, *Spartina alterniflora*, at Sapelo Island, GA during the summers of 2018,
129 2019 and 2020. A combination of prokaryotic DNA and RNA quantification, shotgun
130 metagenomics, metatranscriptomics, and rate measurements of two key pathways of the nitrogen
131 cycle were performed along a stress gradient within three compartments: sediment, rhizosphere
132 and root (Figure 1). The short and tall *S. alterniflora* phenotypes represent the end extremes of the
133 plant biomass gradient formed by stress from salinity, sulfide toxicity and anoxia (Figure 1). Four
134 biological replicates per compartment and *S. alterniflora* phenotype were sequenced for both

135 metagenomic and transcriptomic analysis (Further details about sequencing in Materials and
136 Methods and Supplementary Table S1).

137 Using a custom-designed bioinformatics pipeline, we binned 239 high-quality metagenome
138 assembled genomes (MAGs; > 50 Quality score). MAGs were dereplicated into 160
139 genomospecies (gsp, plural: gspp) by grouping them according to 95% average nucleotide identity
140 (ANI) (Figure 2). MAGs were assigned to 19 phyla. Almost half of the recovered genomes were
141 taxonomically affiliated with the *Proteobacteria* or *Desulfobacterota* phyla (Figure 2, further
142 MAGs taxonomic and statistical information in Supplementary Table S2). Taxonomic novelty was
143 assessed using GTDB-Tk v2.1.0 with the reference database R07-RS207 (Chaumeil et al., 2022).
144 Recovered MAGs included 1 gspp from a previously undescribed order, 10 gspp from undescribed
145 families, 52 gspp from undescribed genera, 94 gspp from undescribed species, and only 3 gspp
146 from previously described species. In order to assess the MAGs' genetic potential to perform
147 important biogeochemical functions in the salt marsh environment, we annotated their open
148 reading frames (ORFs) using the eggNOG database, and focused on predicted genes involved in
149 the biogeochemical cycling of carbon, nitrogen, and sulfur (Supplementary Table S3).

150 A large proportion of binned *Proteobacteria*, including members of the *Ca.* Thiodiazotropha
151 genus, contained genes for nitrogen fixation, carbon fixation through RuBisCO, as well as for
152 dissimilatory sulfur metabolism, and thiosulfate oxidation using the soxABXYZ complex (Figure
153 2). Most MAGs from the *Desulfobacterota* phylum presented genes for dissimilatory metabolism
154 of sulfur, including members of the *Desulfosarcinaceae* family (Figure 2). Because the
155 dissimilatory sulfite reductase enzyme (dsrAB) can function in either sulfur reduction or oxidation,
156 we performed a phylogenetic analysis to identify the dsrAB type from our MAGs. We aligned
157 recovered dsrAB genes to a reference alignment (Müller et al., 2015) and annotated the dsrAB

158 type based on placement in an approximately-maximum-likelihood phylogenetic tree
159 (Supplementary Figure S1). All dsrAB genes retrieved from *Proteobacteria* gspp (*Alpha*- and
160 *Gammaproteobacteria* gspp) were placed within the oxidative type; while dsrAB genes recovered
161 from *Acidobacteriota*, *Bacteroidota*, *Chloroflexota*, *Desulfobacterota*, *Gemmatimonadota*, and
162 *Nitrospirota* gspp clustered within the reductive bacterial dsrAB type (Supplementary Figures S1,
163 S2).

164 We measure rates of $^{15}N_2$ fixation under oxic and anoxic conditions by sediment, a rhizosphere-
165 root mix, and root samples. Rates were measured under oxic and anoxic conditions to capture the
166 oxygen fluctuation experienced by microorganisms in the root-zone of *S. alterniflora*. The two *S.*
167 *alterniflora* phenotypes exhibited significantly higher N fixation rates in their root tissue compared
168 to the sediment or rhizosphere-root mix under both aerobic and anaerobic conditions (Figure 3).
169 Root tissue from the stressed short *S. alterniflora* phenotype showed 1.9- and 5.1-times greater N
170 fixation rates than roots of the tall phenotype under aerobic and anaerobic conditions, respectively
171 (Figure 3). Conversely, sediment from the tall *S. alterniflora* phenotype presented greater potential
172 nitrification rates between one and two orders of magnitude than all other studied compartments
173 (Figure 3). In the short *S. alterniflora*, potential nitrification rates were an order of magnitude
174 greater in root tissue compared to bulk and rhizospheric sediment (Figure 3).

175 We used metagenomic and metatranscriptomic short reads to relate nitrogen fixation activity with
176 multi-omics functional information. Metagenomic and metatranscriptomic reads were functionally
177 annotated using the eggNOG database. We normalized the functional profile of each library to
178 account for differences in sequencing effort and genome size by dividing the count matrix against
179 the median abundance of 10 universal single-copy phylogenetic marker genes as in Salazar et al.
180 (2019). Statistical difference between the normalized gene expression of the nitrogenase gene nifK

181 and the oxidative and reductive dsrA types was calculated between *S. alterniflora* phenotypes
182 across all compartments. Since gene expression within metabolic pathways was highly correlated,
183 we used nifK and dsrA as marker genes (Supplementary Figure S3). Even though nitrogen fixation
184 rates were the greatest in the root compartment of the short *S. alterniflora* phenotype, no statistical
185 significance was found in the nitrogenase gene expression between the two *S. alterniflora*
186 phenotypes (Figure 3). Conversely, the root compartment of the short *S. alterniflora* phenotype
187 had the highest normalized transcript abundance of both reductive and oxidative dsrA gene types
188 (Figure 3). To infer which members of the *S. alterniflora* root microbiome contributed the most to
189 nitrogen fixation, as well as to test if nitrogen fixation was coupled to sulfur metabolism, we
190 mapped all short read transcripts annotated as nifK and dsrA back to our binned gspp. Sulfur-
191 oxidizing *Ca.* Thiodiazotropha gspp in the short phenotype of *S. alterniflora* contributed
192 approximately 25% and 15% of all oxidative dsrA and nifK transcripts, respectively (Figure 3). In
193 addition, the most active sulfur-oxidizing and sulfate-reducing gspp in roots of the short phenotype
194 (gsp 31 and gsp 68) had a positive correlation between nitrogen fixation and sulfur
195 oxidation/reduction gene expression, respectively (Supplementary Figure S4). In the tall
196 phenotype, *Desulfosarcinaceae* gsp 134 contributed the most transcripts of the reductive dsrA
197 gene. However, in general, we were not able to recover most of the nifK genes as part of the
198 MAGs; and thus, transcripts, presumably due to issues with contig binning. Nevertheless, using
199 short read analysis, we found that the majority of the nifK transcripts in the roots of the tall
200 phenotype were assigned to bacteria from the *Desulfobacterota* phylum, while in the short
201 phenotype most nifK transcripts were affiliated with bacteria from the *Gammaproteobacteria* class
202 or the *Desulfobacterota* phylum (Supplementary Figure S5). Similarly, abundant transcripts of
203 oxidative dsrA in the roots of the short phenotype were mostly affiliated with the

204 *Gammaproteobacteria* class, while the reductive dsrA affiliated mainly with the *Desulfobacterales*
205 and *Desulfovibrionales* orders in both phenotypes (Supplementary Figures S6 and S7).

206 2.2 Phylogeny, genetic potential and gene expression of microorganisms enriched in the *S.*
207 *alterniflora* root microbiome

208 To assess the phylogenetic novelty and relation of *Sedimenticolaceae* sulfur-oxidizing MAGs from
209 the present study in comparison to that of marine invertebrate chemosymbionts, we retrieved all
210 publicly available *Sedimenticolaceae* genomes as reported by GTDB release R07-RS207, as well
211 as all *Ca.* Thiodiazotropha spp. analyzed by Osvatic et al. (2023). A maximum-likelihood
212 phylogenetic tree using a 400 universal marker genes database was performed in PhyloPhlAn. We
213 found that *S. alterniflora* root symbionts assigned to the *Ca.* Thiodiazotropha genus and an
214 unknown genus from the *Sedimenticolaceae* family formed a monophyletic clade with lucinid
215 clam chemosymbionts (Figure 4). All recovered MAGs that were phylogenetically related to
216 marine invertebrate chemosymbionts were highly abundant in the root compartment of the *S.*
217 *alterniflora* short phenotype, where sulfidic conditions are found in the marsh environment (Figure
218 1). To conserve phylogenetic coherence, we propose that *S. alterniflora* root symbionts assigned
219 to the *Sedimenticolaceae* family and that formed a monophyletic group with *Ca.* Thiodiazotropha
220 spp. are also members of such genus (Figure 4). Out of the 7 recovered *Ca.* Thiodiazotropha gspp,
221 6 had genes for carbon fixation (RuBisCO), 5 had the complete or partial nifDKH nitrogenase
222 genes for nitrogen fixation, and all of them harbor the complete or at least partial genes for
223 dissimilatory sulfite reductase (oxidative dsrAB type), and sulfur oxidation by the SOX complex
224 (soxABYXYZ). Furthermore, we calculated the gene expression profile of the most active *Ca.*
225 Thiodiazotropha gspp (gsp 31 and gsp 33), finding that genes for sulfur oxidation through the
226 oxidative dsrAB, soxABYXYZ complex, and cytochrome c oxidase cbb3-type genes, as well as

227 genes for carbon and nitrogen fixation (RuBisCO and nifKDH) were among the most highly
228 transcribed (Supplementary Tables S4 and S5). We also found that sulfate-reducing MAGs from
229 the *Desulfosarcinaceae* family were enriched in the root compartment of *S. alterniflora*
230 (Supplementary Figure S8). *Desulfosarcinaceae* gspp had contrasting preferences for root
231 colonization, with gsp 68 mostly enriched in the roots of the short phenotype, gsp 134
232 preferentially enriched in the root of the tall phenotype, and gsp 80 equally abundant in both
233 phenotypes (Supplementary Figure S8). Of the three *Desulfosarcinaceae* gspp, all contained the
234 complete or partial genes for nitrogen fixation, and only gsp 80 did not have the reductive dsrAB
235 gene. The most transcribed genes from both gsp 68 and gsp 134 were related to dissimilatory
236 sulfate reduction (dsrAB and aprAB, Supplementary Tables S6 and S7).

237 2.3 Sediment and root microbiomes have contrasting functional profiles across a salt marsh
238 primary productivity gradient

239 A decreasing trend in prokaryotic alpha divestity was observed from the sediment compartment to
240 the root tissue in both *S. alterniflora* phenotypes (Figure 5). Similarly, quantification of the 16S
241 rRNA gene by qPCR showed statistically lower prokaryotic abundance in the root tissue compared
242 to the sediment and rhizosphere compartments (Figure 5). A stronger barrier for prokaryotic root
243 colonization, evidenced by a steeper decrease in prokaryotic abundance in the rhizosphere-root
244 interface, was observed in the less stressed tall *S. alterniflora* phenotype (Figure 5). Conversely,
245 the root compartment of both *S. alterniflora* phenotypes presented a higher transcript copy number
246 of the prokaryotic 16S rRNA than their sediment counterparts, indicating greater prokaryotic
247 activity in the root zone (Figure 5).

248 PERMANOVA and principal coordinate analysis from metagenomic and metatranscriptomic
249 functional profiles indicated that the environmental stress gradient significantly affects the
250 microbiome's potential and expressed functional repertoire (Figure 5, Supplementary Table S8).

251 The community-level abundance and expression of terminal oxidase genes for aerobic respiration
252 were specific to compartment and *S. alterniflora* phenotype. The relative abundance of genes for
253 the canonical cytochrome c oxidase system (coxA) was greater in the tall *S. alterniflora* phenotype
254 in both metagenomic and metatranscriptomic samples, while cbb3-type cytochrome c genes
255 (ccoN) were mostly present and transcribed in the root tissue of the short *S. alterniflora* phenotype
256 (Figure 5). Genes related to the redox cycling and turnover of nitrogen were more abundant and
257 transcribed in the sediment of the tall *S. alterniflora* phenotype than all other assessed marsh
258 compartments [i.e., nitrification, denitrification, and dissimilatory nitrate reduction to ammonium
259 (DNRA) genes] (Figure 5). Conversely, genes for prokaryotic carbon fixation by RuBisCO and
260 nitrogen fixation had the greatest relative abundance in the root compartment, especially in those
261 from the short *S. alterniflora* phenotype (Figure 5). Nevertheless, relative gene expression for
262 nitrogen fixation was greater in the sediment from the short phenotype and contributed mostly by
263 cyanobacteria species (Supplementary Figure S5). Finally, greater redox cycling of sulfur in the
264 root compartment, especially in the short *S. alterniflora,* was evidenced by the abundance and
265 expression of sulfur dissimilatory metabolism genes (Figure 5).

266 <u>2.4 Plant species from coastal marine ecosystems harbor unique root microbiomes</u>

267 In order to understand how root microbiomes are assembled in coastal marine ecosystems
268 compared to better-studied terrestrial plants, we used publicly available sequences to generate and
269 curate a 16S rRNA gene amplicon database from root microbiomes comprising 2,911 amplicon
270 samples from 56 plant species (complete dataset in Supplementary Table S9). We grouped
271 amplicon samples into 4 broad ecosystem types: seabed, coastal wetlands, freshwater wetlands,
272 and other terrestrial ecosystems. Species exchange based on the Bray-Curtis dissimilarity matrix
273 was largely explained by ecosystem type, with coastal wetland and seabed ecosystems clustering

274 together in an NMDS ordination (Figure 6). PERMANOVA analysis revealed that ecosystem type
275 alone significantly explained 13.2% of the variation of the species exchange between analyzed
276 samples (Supplementary Table S10). Furthermore, to explore two functional guilds that may
277 explain the difference in microbiome assembly between ecosystem types, we assigned putative
278 sulfate reduction and sulfur oxidation functions to our taxonomy table as performed by Rolando
279 et al. (2022). We found that the root microbiomes of both seabed and coastal wetland ecosystems
280 were highly enriched in putative sulfate-reducing and sulfur-oxidizing bacteria (Figure 6).
281 Furthermore, we discovered that in both seabed and coastal wetland ecosystems, amplicons
282 showing high sequence identity to known sulfur-oxidizing bacteria with the capability for nitrogen
283 fixation (*Sedimenticolaceae* family: *Ca.* Thiodiazotropha genus) were highly abundant
284 (Supplementary Figure S9). Conversely, amplicons showing high sequence identity to sulfate
285 reducers from the *Desulfosarcinaceae* family, particularly those from the genus *Desulfatitalea*
286 were highly enriched in the roots of coastal wetland plants (Supplementary Figure S9). The
287 taxonomic identity of highly abundant ASVs in the root compartment of coastal marine plants
288 coincide with diazotrophic MAGs retrieved from Sapelo Island, GA, such as sulfur oxidizers of
289 the *Sedimenticolaceae* family, and sulfate reducers of the *Desulfosarcinaceae* family.

290 **3. Discussion**

291 3.1 Nitrogen fixation is stimulated by rapid sulfur cycling in the roots of *S. alterniflora*

292 Nitrogen fixation in belowground coastal vegetated ecosystems has been mainly associated with
293 heterotrophy, and particularly with sulfate reduction (Gandy and Yoch, 1988; McGlathery et al.,
294 1998; Herbert, 1999; Nielsen et al., 2001; Welsh et al., 1996). The linkage of sulfate reduction to
295 nitrogen fixation was proposed based on studies quantifying rates of diazotrophy with and without
296 sulfate reduction inhibition by molybdate. Here, we show for the first time that highly-abundant

297 sulfur-oxidizing bacteria in the roots of *S. alterniflora* also encode and highly express genes for
298 nitrogen fixation (Figure 2, Figure 3). Furthermore, the MAG with the highest nitrogenase gene
299 expression in our study was a novel sulfur-oxidizing bacterium from the *Ca.* Thiodiazotropha
300 genus that also showed high expression of sulfur oxidation genes (Figure 3, Supplementary Figure
301 S4). Our results suggest that when sulfate reduction was inhibited in previous studies, it disrupted
302 the redox cycling of sulfur by impeding the flow of reduced sulfur compounds that serve as an
303 energy source for sulfur-oxidizing bacteria. Thus, most likely previous inhibition studies not only
304 blocked nitrogen fixation from sulfate-reducing microorganism, but also significantly reduced
305 nitrogen fixation coupled to sulfur oxidation. Unlike sulfate reduction, there is no reliable method
306 for measuring sulfide oxidation rates. Thus, the abundance and expression of sulfur-oxidation
307 genes is one of the few ways to directly link this otherwise unmeasurable process with nitrogen
308 fixation. We propose that both dissimilatory sulfur reduction and oxidation, and more importantly,
309 the rapid redox cycling of sulfur, stimulate nitrogen fixation in the root environment of *S.*
310 *alterniflora*. Since coastal wetland plants and seagrasses assemble similar root microbiomes
311 (Figure 6), and macrophyte activity boosts both nitrogen fixation and the cycling of sulfur, this
312 may be a common phenomenon in the root zone of many coastal marine plants (Whiting et al.,
313 1986; McGlathery et al., 1998; Welsh et al., 1996).

314 Further evidence supporting the significance of the rapid cycling of sulfur coupled to nitrogen
315 fixation is that members of the *Gammaproteobacteria* class and *Desulfobacterota* phylum
316 contributed most of the nitrogenase and oxidative/reductive dsrAB transcripts in the root
317 compartment of *S. alterniflora*. Similar results have been obtained from DNA and RNA amplicon
318 studies in seagrass and other coastal wetland plant species, where nitrogen fixation genes and their

319 expression have been affiliated with microorganism closely related to sulfate-reducing and sulfur-
320 oxidizing bacteria (Thomas et al., 2014; Crump, et al. 2018; Kolton et al., 2020).

321 3.2 The root zone of coastal marine ecosystems is a hotspot of sulfur redox cycling

322 In most coastal marine ecosystems, water saturated sediments are depleted in oxygen within the
323 first millimeters depth (Jørgensen et al., 2019). Because coastal marine ecosystems are bathed in
324 seawater containing high sulfate concentrations (28 mM), sediment sulfate-reducing
325 microorganisms often perform the terminal step of organic matter decomposition (Jørgensen et al.,
326 2019). Unlike aerobic respiration, energy flow during sulfate reduction is decoupled from the
327 carbon cycle, with most of the free energy conserved in reduced sulfur compounds (Howarth,
328 1984). The chemically stored energy is subsequently released by biotic and abiotic oxidation
329 reactions at marsh oxic-anoxic interfaces coupled to the reduction of potent electron acceptors
330 (oxygen, nitrate, or oxidized metals) (Howarth, 1984). Surface sediments of vegetated coastal
331 marine ecosystems experience rapid re-oxidation of most reduced sulfur compounds. This process
332 is highly concentrated in the microaerophilic root zone, which serves as a hotspot for the reaction
333 (Holmer et al., 2002; Kristensen and Alongi, 2006; Koop-Jakobsen et al., 2018). Our results
334 showing that the root compartment of coastal marine ecosystems is highly enriched in
335 microorganisms with the capability for both sulfur reduction and oxidation provides further
336 evidence for rapid sulfur cycling in the root zone (Figure 6). Furthermore, to the best of our
337 knowledge, this is the first study to employ genome reconstruction from metagenomic sequencing
338 to verify the function of uncultivated sulfate-reducing and sulfur-oxidizing microorganisms living
339 in the roots of coastal wetland plants. Our findings also reveal that genes that catalyze oxidative
340 and reductive reactions in the sulfur cycle are highly transcribed in the root environment,
341 particularly in the stressed *S. alterniflora* phenotype that thrives in a sulfidic environment (up to

342 1.5 mM sulfide concentration in our studied transects; Rolando et al. 2022). This is consistent with
343 previous studies of salt marsh and seagrass ecosystems, in which genes of sulfur-oxidation
344 pathways were shown to be highly expressed in the root compartment of *S. alterniflora* and *Zostera*
345 seagrass spp., respectively (Thomas et al. 2014, Crump et al., 2018). Thus, we propose that in
346 contrast to terrestrial ecosystems, coastal marine plants rely on the rapid cycling of sulfur in their
347 root zone for the breakdown of organic matter and recycling of nutrients through sulfate reduction
348 along with the re-oxidation of terminal electron acceptors by sulfur oxidation. Furthermore, we
349 propose that rapid rates of both oxidative and reductive sulfur reactions represent a key mechanism
350 to sustain high rates of energetically-expensive nitrogen fixation in the root zone of *S. alterniflora*.

351 3.3 Phylogenetic and ecological relationship between marine invertebrates and *S. alterniflora*
352 chemosymbionts

353 Endosymbionts from the *Ca.* Thiodiazotropha genus were initially discovered living in symbiosis
354 with lucinid clams, where they fix carbon and serve as a source of carbon and nitrogen to the
355 animal host using energy gained from the oxidation of reduced forms of sulfur (Petersen et al.,
356 2017). Recent studies using fluorescence in situ hybridization (FISH) microscopy and SSU rRNA
357 gene metabarcoding have shown that *Ca.* Thiodiazotropha bacteria also inhabit the roots of a
358 diverse array of seagrass species along with that of the coastal cordgrass *S. alterniflora* (Martin et
359 al., 2020a; Rolando et al., 2022). Here, we show that close relatives of diazotrophic sulfur
360 chemosymbionts associated with lucinid clams were highly abundant and active in the roots of *S.*
361 *alterniflora*. To the best of our knowledge, this is the first study reporting genomes and gene
362 expression profiles from *Ca.* Thiodiazotropha retrieved from macrophyte root samples. We show
363 that our MAGs formed a monophyletic clade with those from previously described marine
364 invertebrate animals (Figure 4). Similar to what has been reported in their symbiosis with lucinid

365 clams, the *S. alterniflora* symbionts highly expressed genes for sulfur oxidation, and carbon and
366 nitrogen fixation (Supplementary Table S4, Supplementary Table S5; Petersen et al., 2017; Lim et
367 al., 2019a). Studies of lucinid clams have shown that the *Ca.* Thiodiazotropha symbionts are
368 horizontally transmitted (Petersen and Yuen, 2021). Furthermore, invertebrate colonization by *Ca.*
369 Thiodiazotropha symbionts is not restricted by either the host or symbiont species (Lim et al.,
370 2019a). The flexibility of this symbiotic relationship could explain the evolution of *Ca.*
371 Thiodiazotropha symbionts colonizing macrophyte roots. Our results show that all *Ca.*
372 Thiodiazotropha symbionts of *S. alterniflora* are distinct species from those previously found in
373 lucinid clam hosts (ANI < 82% for all pairwise comparisons). However, additional metagenomic
374 sequencing of both macrophyte plants and lucinid clams is needed to better interrogate if
375 chemosymbionts populations are restricted by host biology at the kingdom level (i.e., to either
376 plant or animal hosts). In contrast to what is observed in lucinid clams, where a single bacterial
377 species dominates the gill microbiome; in *S. alterniflora* and seagrass species, *Ca.* Thiodiazotropha
378 spp. do not completely outcompete other microbial species in the root compartment (Lim et al.,
379 2019a, 2019b). However, the symbionts comprise a large proportion of the microbial community,
380 and are amongst the most active species (Rolando et al., 2022; Supplementary Figure S9).

381 3.4 Sulfur chemosymbiosis as an adaptation to anoxia and sulfide toxicity in *S. alterniflora* plants

382 We propose that the symbiosis between *S. alterniflora* and sulfur-oxidizing bacteria represents a
383 key adaptation supporting the resilience of coastal salt marsh ecosystems to environmental
384 perturbations. For instance, intertidal wetland ecosystems are vulnerable to climate change because
385 they are located in a narrow elevation range determined by tidal amplitude (Morris et al., 2021).
386 The Intergovernmental Panel on Climate Change (IPCC) has projected an increase in sea level
387 between 0.38 m and 0.77 m by 2100 (IPCC-AR6, Fox-Kemper et al., 2021). Although coastal

388 wetland ecosystems are dynamic and adapt to sea level rise by increasing sediment accretion rates,
389 ecosystem models predict that a large area of present-day marsh will drown because of accelerated
390 sea level rise (Kirwan et al., 2016). Increased hydroperiods will impact the redox balance of
391 vegetated sediments, imposing more severe anoxia and physiological stress from sulfide toxicity
392 to wetland plants. Under this scenario, a symbiosis of coastal vegetated plants with sulfur-
393 oxidizing bacteria could alleviate sulfide stress while at the same time coupling it to carbon and
394 nitrogen fixation for potential plant uptake; however, the mechanism for carbon and/or nitrogen
395 transfer between sulfur-oxidizing symbionts and the host plants still remains elusive and requires
396 further research. Similar to Thomas et al. (2014), we showed the transcription of sulfur oxidation
397 genes was greater in the stressed *S. alterniflora* short phenotype. In seagrass ecosystems, Martin
398 et al. (2020b) also found that the seagrass root microbiome was more enriched in *Ca.*
399 Thiodiazotropha spp. under stress conditions. Thus, we suggest that the *S. alterniflora – Ca.*
400 Thiodiazotropha symbiosis is an adaptive interaction to anoxic soil conditions, whereby the host
401 plant responds to stress from elevated dissolved sulfide concentrations. Further, we show that the
402 short *S. alterniflora* phenotype, which harbors a greater nitrogenase transcript abundance of *Ca.*
403 Thiodiazotropha sulfur chemosymbionts, also had the greatest rates of N fixation of all assessed
404 marsh compartments. Our results support the SGH in which greater stress strengthens the
405 relationship between sulfur oxidizing bacteria and macrophyte plants. Stressed plants benefit from
406 the symbiotic relationship through reduced sulfide toxicity and the coupling of sulfide oxidation
407 to nitrogen fixation, with nitrogen likely transferred to the plant host. Conversely, the tall *S.*
408 *alterniflora* phenotype showed a faster internal cycling of nitrogen, which is consistent with
409 previous studies showing greater rates of nitrogen mineralization in this zone of the ecosystem
410 (Figure 5, Rolando et al., 2022).

411 Intriguingly, we also found high transcript expression of RuBisCO from *Ca.* Thiodiazotropha gspp
412 in the root compartment of the stressed short phenotype of *S. alterniflora* (Supplementary Table
413 S5). When assessing the natural abundance of ^{13}C ($\delta^{13}C$) in the roots of the short *S. alterniflora*,
414 we found that it was significantly depleted compared to the $\delta^{13}C$ from the tall phenotype
415 (Supplementary Figure S10). As a C4 plant, *S. alterniflora* first fixes carbon by the action of PEP
416 carboxylase, which has lower discrimination against ^{13}C than RuBisCO (Farquhar, 1983). Thus,
417 we could speculate that the higher ^{13}C discrimination in the root of the short *S. alterniflora*
418 phenotype is a consequence of sulfur chemoautotrophic carbon fixation by RuBisCO. Consistent
419 with our hypothesis, a previous study by Hwang and Morris (1992) showed that the roots of *S.*
420 *alterniflora* fix carbon through an undeciphered dark reaction. Further, unlike other plant species,
421 *S. alterniflora* assimilates sulfur as sulfide (Carlson and Forrest, 1982), and under mild sulfidic
422 conditions, sulfur oxidation in *S. alterniflora* roots is mostly biological and was previously
423 hypothesized to be coupled with energetic gain (Lee et al., 1999). Interestingly, low doses of
424 sulfide (< 1 mM) have been shown to stimulate the productivity of *S. alterniflora* (Mendelssohn
425 and Morris, 2000). However, since other plant physiological processes could also explain
426 differences in $\delta^{13}C$, such as differing rates of dark respiration, and leakiness from the bundle sheath
427 cells to the mesophyll cell (Farquhar, 1983), further investigations are required to quantify the
428 relevance of sulfur chemolithoautotrophy in *S. alterniflora* root biomass production.

429 **4. Materials and methods**

430 <u>4.1 Study site, field sampling and sample processing</u>

431 The field fraction of this study was carried out in the Georgia Coastal Ecosystem - Long Term
432 Ecological Research (GCE-LTER) site 6, located on Sapelo Island, GA (Lat: 31.389° N, Long:
433 81.277° W). Four ~100 m transects along the tall to short *Spartina alterniflora* gradient were

434 studied in July 2018, 2019, and 2020 (Figure 1, further site description in Rolando et al., 2022). A
435 combination of multi-omics approaches and biogeochemical rate measurements were performed
436 across different salt marsh compartments and phenotypes of *S. alterniflora*.

437 The microbiome of *S. alterniflora* was analyzed using shotgun metagenomics from three
438 compartments: sediment, rhizosphere, and root. The tall and short *S. alterniflora* extremes of the
439 four studied transects were sampled (n: 4 transects * 2 *S. alterniflora* phenotypes * 3 compartments
440 = 24). Samples from transects 1 and 2 were collected in July 2018, while those from transects 3
441 and 4 were collected in July 2019. All sampling was performed at the 0-5 cm depth profile. Root-
442 associated samples were washed two times with creek water in the field to remove coarse chunks
443 of sediment attached to the plant. All samples were immediately flash-frozen in an ethanol and dry
444 ice bath, and stored at -80ºC until DNA extraction.

445 Samples for metatranscriptomic analysis and biogeochemical rate measurements were collected in
446 July 2020 only from transect 4 to reduce plant disturbance time before flash freezing and
447 incubations, respectively. Five independent plants at least 3 meters apart were sampled with a
448 shovel at the two *S. alterniflora* biomass extremes. The entire plant, including the undisturbed root
449 system with sediment attached, was sampled up to at least 20 cm depth, transferred to a 5 gallons
450 bucket, and immediately transported to the field lab. For each plant, a paired sample of sediment
451 was collected. In the lab, roots were washed with creek water two times. After the first wash, roots
452 with sediment attached were collected and defined as the rhizosphere + root compartment. Live,
453 sediment-free roots were sampled after the second wash and defined as the root compartment. Top
454 5 cm from each sample were homogenized and used for total RNA extractions and measurements
455 of nitrogen fixation and potential nitrification rates. Root samples for RNA extractions were
456 washed in an epiphyte removal buffer, as in Simmons et al. (2018). Sediment and root samples for

457 RNA analysis were immediately flash-frozen in an ethanol dry ice bath, and stored at -80 ºC until
458 extraction. Due to limited sample amount, we did not prepare rhizosphere libraries for
459 metatranscriptomic analysis.

460 4.2 Nitrogen fixation and potential nitrification rates

461 Rates of N fixation were calculated in $^{15}N_2$ incubations in 14 ml serum vials as in Leppänen et al.
462 (2013). Rates were measured for all samples under both oxic and anoxic conditions. About 2 g,
463 and 1 g of wet weight was used for tracer gas incubations of sediment and root samples,
464 respectively. An additional subsample of 2 g was immediately oven-dried at 60 ºC for 72 hours to
465 be used as a pre-incubation control. In all vials containing root samples, 4 ml of autoclaved and
466 0.22 um filter-sterilized artificial seawater was added to avoid tissue desiccation. No artificial
467 seawater was added to sediment and rhizosphere samples since they were already water-saturated.
468 In anoxic incubations, vials were flushed with N_2 gas for 5 minutes. After sealing all incubation
469 vials, 2.8 ml of gas was removed and immediately replaced with 2.8 ml of $^{15}N_2$ (98% enriched,
470 Cambridge Isotope Laboratories Inc, USA). Vials were overpressured by adding 0.3 ml of air or
471 N_2 gas in oxic or anoxic incubations, respectively. The incubations were carried out in the dark
472 and at room temperature for 24 hours. At the end of the incubation, samples were oven dried at 60
473 ºC for 72 hours, and ground using a PowerGen high throughput homogenizer (Fisherbrand,
474 Pittsburgh, PA). Ground samples were sent to the University of Georgia Center for Applied Isotope
475 Studies (https://cais.uga.edu/) for carbon and nitrogen elemental analysis and ^{13}C and ^{15}N stable
476 isotope analysis. Elemental analysis was performed by the micro-Dumas method, while isotopic
477 analysis by isotope ratio mass spectrometry. Rates of ^{15}N incorporation were calculated per dry
478 weight basis (DW) as in Leppänen et al. (2013):

479 N uptake rate $\left(\text{nmol g}^{-1}\text{ DW h}^{-1}\right)=$

480 $$\frac{\frac{1}{100}\times\frac{\%N}{100}\times\left[\frac{\text{atom}\%_{\text{sample}}\text{-atom}\%_{\text{control}}}{MW(N_2)}\right]\times 10^9\times\frac{100}{\text{atom}\%_{\text{headspace}}}}{\text{hours}} \qquad [1]$$

481 Where %N is the N percent concentration of the oven-dried sample, and $MW(N_2)$ is the molecular
482 weight of N_2 (28.013446).

483 Potential nitrification rates were measured as detailed by Dollhopf et al. (2005) in 5 replicates for
484 each tall and short *S. alterniflora* compartments: sediment, rhizosphere + root, and root.
485 Homogenized samples (5 g, 5 g, and 2 g for sediment, rhizosphere + root, and root compartment,
486 respectively) were placed in 250-ml Erlenmeyer flasks filled with 50 ml sterile artificial seawater.
487 Sodium chlorate and ammonium sulfate were amended to all flasks to final concentrations of 10
488 mM and 500 µM, respectively. Flasks were incubated in the dark at room temperature and orbital
489 shaking (115 rpm) for 24 hours. Subsamples for NO_2 analysis were taken at 0, 4, 8, 12, 18, and 24
490 hours. Timepoint samples were filtered with 0.2 µm syringe filters, and stored at -20 ºC until
491 analysis. Filtered NO_2 concentration was measured by spectrophotometry (García-Robledo et al.,
492 2014). Potential nitrification rates (N nmol g^{-1}_{DW} h^{-1}) were calculated as the slope of the linear
493 regression of NO_2 concentration over time.

494 <u>4.3 Nucleic acid extractions and multi-omics library preparation</u>

495 For DNA extractions, compartment separation of the rhizosphere and root microbiomes was
496 performed by sonication in an epiphyte removal buffer, as detailed in Simmons et al. (2018).
497 Extracellular dissolved or sediment-adsorbed DNA was removed from bulk sediment samples
498 according to the Lever et al. (2015) procedure. DNA extractions from all samples were performed
499 using the DNeasy PowerSoil kit (Qiagen, Valencia, CA) following the manufacturer's instructions.

500 Shotgun metagenome sequencing was performed on an Illumina NovaSeq 6000 S4 2x150 Illumina
501 flow cell at the Georgia Tech Sequencing Core (Atlanta, GA).

502 RNA from 4 biological replicates of both the sediment and root compartments from the tall and
503 short phenotypes of *S. alterniflora* was extracted using the ZymoBIOMICS RNA Miniprep (Zymo
504 Research Corp) kit according to the manufacturer's protocol (n: 4 replicates * 2 *S. alterniflora*
505 phenotypes * 2 compartments = 16 samples). Rigorous DNA digestion was done with the TURBO
506 DNase kit (Invitrogen), and eukaryotic mRNA was removed by binding and discarding the
507 eukaryotic mRNA polyA region to oligo d(T)25 magnetic beads (England Biolabs). Finally, rRNA
508 from both plant and prokaryotic organisms was depleted using the QIAseq FastSelect -rRNA Plant,
509 and -5S/16S/23S kits, respectively (Qiagen, Valencia, CA). Metatranscriptomic libraries were
510 sequenced in two lanes of Illumina's NovaSeq 6000 System flow cell utilizing the NovaSeq Xp
511 workflow (SE 120bp) at the Georgia Tech Sequencing Core (Atlanta, GA). We retrieved 203, and
512 415 Gpb of metagenomic and metatranscriptomic raw sequences, respectively; with a median
513 sequencing effort of 7.8, and 25.3 Gbp per metagenomic and metatranscriptomic library
514 (Supplementary Table S1). After quality control and *in silico* removal of host and rRNA reads,
515 median sequencing effort decreased to 5.3 and 9 Gbp per metagenomic and metatranscriptomic
516 library, respectively (Supplementary Table S1).

517 <u>4.4 Gene and transcript quantification of the prokaryotic 16S rRNA gene</u>

518 Prokaryotic abundance and a proxy of prokaryotic activity were measured by quantitative
519 polymerase chain reaction (qPCR) and Reverse Transcription-qPCR (RT-qPCR) of the SSU rRNA
520 gene, respectively. All samples used for metagenome and metatranscriptome analysis were
521 quantified by qPCR and RT-qPCR, respectively. Samples were analyzed in triplicate using the
522 StepOnePlus platform (Applied Biosystems, Foster City, CA, USA) and PowerUp SYBR Green

523 Master Mix (Applied Biosystems, Foster City, CA, USA). Reactions were performed in a final
524 volume of 20µl using the standard primer set for the prokaryotic SSU rRNA gene: 515F (5′-
525 GTGCCAGCMGCCGCGGTAA′) and 806R (5′-GGACTACHVGGGTWTCTAAT′) (Caporaso
526 et al., 2011, Rolando et al., 2022). To avoid plant plastid and mitochondrial DNA/cDNA
527 amplification from root samples, peptide nucleic acid PCR blockers were added to all qPCR and
528 RT-qPCR reactions at a concentration of 0.75 µM (Lundberg et al., 2013). Standard calibration
529 curves were performed using a 10-fold serial dilution (10^3 to 10^8 molecules) of standard pGEM-T
530 Easy plasmids (Promega, Madison, WI, USA) containing target sequences from *Escherichia coli*
531 K12. Melting curve analyses was used to check for PCR specificity. Prokaryotic gene and
532 transcript abundance of the SSU rRNA gene were calculated as gene and transcript copy number
533 g^{-1} of fresh weight, respectively.

534 4.5 Metagenomic and metatranscriptomic quality control

535 Metagenomic and metatranscriptomic raw reads were quality trimmed (quality phred score < 20),
536 and filtered for Illumina artifacts, PhiX, duplicates, optical duplicates, homopolymers, and
537 heteropolymers using JGI's BBTools toolkit (Bushnell, 2014). Reads shorter than 75 bp were
538 removed, and the quality of both metagenomic and metatranscriptomic libraries was assessed with
539 FastQC (Andrews, 2010). Remaining reads were mapped against the only publicly available *S.*
540 *alterniflora* genome (NCBI BioProject: PRJNA479677) with bowtie2 (Langmead and Salzberg,
541 2012), followed by removal of short reads that aligned to the *S. alterniflora* genome using samtools
542 (parameters: view -u -f 12 -F256, Li et al., 2009). In addition, rRNA reads from metatranscriptomic
543 samples were removed using sortMeRNA v.4.3.4 (Kopylova et al., 2012). Finally, DNA
544 contamination in metatranscriptomic samples was assessed as indicated by Johnston et al. (2019).
545 Short-read transcripts were mapped to all assembled contigs, and strand-specificity (consistency

546 in sense/antisense orientation) was calculated for all genes with more than 100 hits. All assessed
547 samples had a greater than 95% average strand-specificity, thus considered to be free of DNA
548 contamination (Supplementary Table S1). Filtered, quality-trimmed, and host-free reads were
549 utilized for subsequent analyses.

550 4.6 Metagenomic and metatranscriptomic short reads functional analysis and nonpareil diversity

551 Short reads from all metagenomic and metatranscriptomic samples were aligned against the
552 eggNOG protein database (release 5.0.2) using eggnog-mapper v.2.1.9 (Cantalapiedra et al., 2021).
553 The DIAMOND tabular outputs were filtered by retrieving only the best hit based on bitscore. Hits
554 with less than 30% identity, less than 30% match of the read length, or that did not match a
555 prokaryotic domain were removed from the analysis. Gene profiles for each metagenomic and
556 metatranscriptomic library were constructed by counting hits of predicted KEGG orthology. Due
557 to differences in sequencing effort and genome size between multi-omics libraries, the count
558 matrixes were normalized by dividing them by their median count of 10 universal single-copy
559 phylogenetic marker genes (K06942, K01889, K01887, K01875, K01883, K01869, K01873,
560 K01409, K03106, and K03110) as in Salazar et al. (2019). Functional gene and transcript profiles
561 were analyzed by an principal coordinate analysis utilizing the Bray-Curtis dissimilarity distance.
562 Further, for both metagenomic and metatranscriptomic profiles, multivariate variation of the Bray-
563 Curtis dissimilarity matrix was partitioned to compartment (sediment, rhizosphere, and root) and
564 *S. alterniflora* phenotype, based on a permutational multivariate analysis of variance
565 (PERMANOVA) with 999 permutations performed in vegan v. 2.5.7 (Oksanen et al., 2013). The
566 normalized relative abundance of selected terminal oxidases and genes/transcripts from the carbon,
567 nitrogen, and sulfur cycles were assessed by compartment and *S. alterniflora* phenotype.

568 After removing reads annotated as Eukaryotic by eggnog-mapper, we calculated nonpareil
569 diversity from all metagenomic samples using nonpareil v. 3.401 (Rodriguez-R et al., 2018b).
570 Nonpareil diversity is a metric estimated from the redundancy of whole genome sequencing reads,
571 and has been shown to be closely related to classic metrics of microbial alpha diversity like the
572 Shannon index.

573 4.7 Recovery of metagenome assembled genomes (MAGs)

574 The following binning approach was motivated by a recently proposed method of iteratively
575 subtracting reads mapping to MAGs, re-assembling, and re-binning metagenomic libraries to
576 increase the number of recovered genomes (Rodriguez-R et al., 2020). An initial assembly using
577 idba-ud v1.1.3 with pre-error-correction for highly uneven sequencing depth was performed for
578 all individual metagenomic libraries (default parameters), as well as co-assemblies grouping
579 libraries from the same *S. alterniflora* phenotype and compartment (--mink 40 --maxk 120 --step
580 20 --min_contig 300) (Peng et al., 2012). The resulting contigs from both individual and co-
581 assemblies were binned using three different algorithms with default options: MaxBin v.2.2.7,
582 MetaBAT v.2.15, and CONCOCT v1.1.0 (Alneberg et al., 2014; Wu et al., 2016; Kang et al.,
583 2019). Recovered bins were dereplicated with DAS Tool v1.1.2 (Sieber et al., 2018), and the output
584 was refined for putative contamination with MAGPurify v2.1.2 (Nayfach et al., 2019).
585 Completeness, contamination, and quality score (Completeness – 5*Contamination) were
586 calculated with MiGA v0.7 (Rodriguez-R et al., 2018a). Recovered MAGs with a quality score
587 less than 50 were considered low quality and discarded. A second round of assembly and binning
588 was performed after discarding short reads that mapped against high-quality (HQ) MAGs.
589 Metagenomic libraries were mapped against HQ MAGs using bowtie2 with default parameters.
590 Paired reads that mapped against HQ MAGs were discarded using samtools (parameters: view -F

591 2, Li et al., 2009). Filtered metagenomic libraries were co-assembled once again using idba-ud
592 v1.1.3 with pre-error-correction for highly uneven sequencing depth (parameters: --mink 40 --
593 maxk 120 --step 20 --min_contig 300) in four groups: i) tall *S. alterniflora* root, ii) short *S.*
594 *alterniflora* root, iii) tall *S. alterniflora* sediment and rhizosphere, and iv) short *S. alterniflora*
595 sediment and rhizosphere. Binning, MAGs' refinement, and quality control were performed as
596 explained for the first iteration. Finally, HQ MAGs from both iterations were grouped into
597 genomospecies (gspp, singular gsp) by clustering MAGs with ANI > 95% using the MiGA v0.7
598 derep_wf workflow (Rodriguez-R et al., 2018a). MAGs with the highest quality score were
599 selected as representatives of their gsp, and most downstream analyses were performed with them.

600 Genomospecies relative abundance was estimated for each metagenomic library as in Rodriguez-
601 R et al. (2020). Sequencing depth was calculated per position using bowtie2 with default
602 parameters (Langmead and Salzberg, 2012), and bedtools genomecov (parameters: -bga, Quinlan
603 and Hall, 2010). Bedtools output was truncated to keep only the central 80% values, and the mean
604 of all retained positions was calculated using BedGraph.tad.rb from the enveomics collection, a
605 metric defined as TAD_{80} (truncated average sequencing depth) (Rodriguez-R and Konstantinidis,
606 2016). Relative abundance of each gsp was calculated by dividing TAD_{80} by genome equivalents
607 estimated for each metagenomic library with MicrobeCensus (Nayfach and Pollard, 2015).

608 <u>4.8 MAGs taxonomy, phylogenetic analysis, and gene functional annotation and expression</u>

609 Taxonomic classification of all MAGs was performed by GTDB-Tk v2.1.0 using the reference
610 database GTDB R07-RS207 (Chaumeil et al., 2022). A maximum likelihood phylogenetic tree of
611 all gspp was constructed using a 400 universal marker genes database in PhyloPhlAn v3.0.58
612 (parameters: -d phylophlan, --msa mafft, --trim trimal, --map_dna diamond, --map_aa diamond, -

613 -tree1 iqtree, --tree2 raxml, --diversity high, --fast, Asnicar et al., 2020). The phylogenetic tree was
614 decorated and visualized in ggtree v2.0.4 (Yu et al., 2018).

615 Protein-encoding genes from all binned MAGs were predicted with Prodigal v.2.6.3 using default
616 parameters (Hyatt et al., 2010), and resulting amino acid sequences aligned against the eggNOG
617 database (release 5.0.2) using eggnog-mapper v2.1.9 (Cantalapiedra et al., 2021). The DIAMOND
618 tabular output was filtered by retrieving only the best hit based on bitscore, and removing hits with
619 less than 30% identity and/or less than 50% match length.

620 Metagenomic and metatranscriptomic short reads were mapped against functionally annotated
621 ORFs of all gspp using megablast v.2.10.1. Only hits with greater than 95% percent identity and
622 90% read alignment were retained. Percent contribution of genes and transcripts to the total
623 microbial community was assessed by dividing the number of hits from each gsp against the total
624 number of functionally annotated short reads (from section 4.7). When assessing the transcript
625 expression profile of a specific gsp, the number of mapped hits per annotated transcript was
626 normalized by dividing it by gene length (bp) and the median abundance of 10 universal single-
627 copy phylogenetic marker genes of the prokaryotic community (K06942, K01889, K01887,
628 K01875, K01883, K01869, K01873, K01409, K03106, and K03110).

629 Finally, since the phylogeny of the dsrAB gene allows to discriminate between the oxidative and
630 reductive dsrAB types, we aligned all recovered genes from our binned gspp to a reference
631 alignment (Müller et al., 2015) with Clustal Omega v.1.2.4 (Sievers et al., 2011), and built an
632 approximately-maximum-likelihood phylogenetic tree with FastTree v.2.1.11 (Price et al., 2010).
633 Gene type was inferred based on placement in the phylogenetic tree.

634 4.9 Phylogenetic reconstruction of the *Sedimenticolaceae* family

635 Publicly available genomes from all species from the *Sedimenticolaceae* family, according to
636 GTDB R07-RS207, and all *Candidatus* Thiodiazotropha genomes from the Osvatic et al. (2023)
637 study were retrieved from NCBI. A full list and characteristics of genomes used for this analysis
638 is found in Supplementary Table S11. A phylogenetic tree of all retrieved genomes and binned
639 genomes from this study was constructed in PhyloPhlAn v3.0.58 using a 400 universal marker
640 genes database (parameters: -d phylophlan, --msa mafft, --trim trimal, --map_dna diamond, --
641 map_aa diamond, --tree1 fasttree, --tree2 raxml, --diversity low, --accurate, Asnicar et al., 2020).
642 The phylogenetic tree was decorated and visualized using ggtree v2.0.4 (Yu et al., 2018).

643 4.10 Analysis of root microbiomes from contrasting ecosystems

644 Publicly available 16S rRNA gene amplicon datasets, generated from next-generation sequencing,
645 were used to characterize the community assembly of root microbiomes from coastal marine
646 ecosystems. Studies were selected based on google scholar queries using a combination of the
647 following keywords: "salt marsh", "coastal", "wetland", "mangrove", "seagrass", "seabed", "crop",
648 "bog", "plant", "root", "endosphere", "microbial community", "microbiome", “amplicon”, “next-
649 generation sequencing”, “16S rRNA”, and “SSU rRNA”, as well as based on the authors prior
650 knowledge. Only studies that collected environmental samples were included (i.e., no greenhouse
651 or plants grown on potting media were included). When available, paired soil/sediment and
652 rhizosphere samples were also retrieved. Twenty-two studies that met our requirements were
653 selected, collecting a total of 2911 amplicon samples, with 1182 of them being from the root
654 compartment across 56 different plant species. Selected plants were categorized into 4 different
655 ecosystem types: seabed, coastal wetlands, freshwater wetlands, and other terrestrial ecosystems.
656 A complete list of selected amplicon samples with accompanying metadata is available in
657 Supplementary Table S9.

658 Cutadapt v.3.7 was used to detect and remove primer sequences from the datasets (Martin, 2011).
659 Primer-free sequences were quality filtered using DADA2's filterAndTrim function [options:
660 truncLen=c(175,150), maxN=0, maxEE=c(2,2), truncQ=10, rm.phix=TRUE] (Callahan et al.,
661 2016). Trimmed reads were randomly subsampled to a maximum of 20,000 reads using seqtk v.1.3
662 (Li, 2012) and used as input for dada2 amplicon sequence variant (ASV) calling (Callahan et al.,
663 2016). Chimeras were removed using the removeBimeraDenovo function from the DADA2
664 package. Taxonomy was assigned to ASVs utilizing the Ribosomal Database Project (RDP) Naive
665 Bayesian Classifier (Wang et al., 2007) against the SILVA SSU rRNA reference alignment
666 [Release 138, (Quast et al., 2012)]. Sequences classified as chloroplast, mitochondrial, and
667 eukaryotic or that did not match any taxonomic phylum were excluded from the dataset. Samples
668 that had less than 5,000 reads were removed at this stage. In order to merge studies from different
669 sequence runs and primer sets, we grouped ASVs at the genus level before merging all studies into
670 a single dataset in phyloseq v.1.36 (McMurdie and Holmes, 2013).

671 Microbial community assembly of the root microbiome was analyzed by performing a non-metric
672 multidimensional scaling (NMDS) ordination utilizing the Bray-Curtis dissimilarity distance.
673 Multivariate variation of the Bray-Curtis dissimilarity matrix was partitioned to ecosystem type,
674 and compartment (soil/sediment, rhizosphere, and root), based on a PERMANOVA with 999
675 permutations performed in vegan v. 2.5.7 (Oksanen et al., 2013). Finally, putative function for
676 sulfate reduction and sulfur oxidation was assigned based on homology at the genus level as in
677 Rolando et al. (2022).

678 **Data availability**

679 Raw metagenomic and metatranscriptomic sequences are deposited in the BioProject database
680 (http://ncbi.nlm.nih.gov/bioproject) under accessions PRJNA703972 and PRJNA950121,

respectively. Metagenome-assembled genomes are found in the BioProject PRJNA703972. Acompanying metadata and custom scripts used in the present study are publicly available in Supplementary Information and in a Zenodo repository: https://doi.org/10.5281/zenodo.7883423

Acknowledgements

This work was supported in part by an institutional grant (NA18OAR4170084) to the Georgia Sea Grant College Program from the National Sea Grant Office, National Oceanic and Atmospheric Administration, US Department of Commerce, and by a grant from the National Science Foundation (DEB 1754756). Any opinions, findings, and conclusions or recommendations expressed in this material are those of the authors and do not necessarily reflect the views of the National Science Foundation.

Author contributions

Conceptualization: J.L.R., M.K., J.T.M., and J.E.K. Field sampling and analysis: J.L.R., M.K., T.S., Y.L., and J.E.K. Bioinformatic analysis: J.L.R., M.K., P.P., R.C., and K.T.K. Funding acquisition: J.E.K. Writing—original draft: J.L.R. with inputs from all authors.

Ethics declarations

The authors declare no competing interests.

References:

1. Alneberg, J., Bjarnason, B.S., De Bruijn, I., Schirmer, M., Quick, J., Ijaz, U.Z., Lahti, L., Loman, N.J., Andersson, A.F. and Quince, C., 2014. Binning metagenomic contigs by coverage and composition. Nature methods, 11(11), pp.1144-1146.
2. Andrews, S., 2010. FastQC: a quality control tool for high throughput sequence data.
3. Asnicar, F., Thomas, A.M., Beghini, F., Mengoni, C., Manara, S., Manghi, P., Zhu, Q., Bolzan, M., Cumbo, F., May, U., Sanders, J.G., 2020. Precise phylogenetic analysis of microbial isolates and genomes from metagenomes using PhyloPhlAn 3.0. Nature communications, 11:1-10.

4. Barbier, E.B., Hacker, S.D., Kennedy, C., Koch, E.W., Stier, A.C. and Silliman, B.R., 2011. The value of estuarine and coastal ecosystem services. Ecological monographs, 81(2), pp.169-193.
5. Bertness, M.D. and Callaway, R., 1994. Positive interactions in communities. Trends in ecology & evolution, 9(5), pp.191-193.
6. Bulgarelli, D., Schlaeppi, K., Spaepen, S., Van Themaat, E.V.L., Schulze-Lefert, P., 2013. Structure and functions of the bacterial microbiota of plants. Annual review of plant biology, 64:807-838.
7. Bushnell, B., 2014. BBTools software package. URL http://sourceforge. net/projects/bbmap.
8. Callahan, B.J., McMurdie, P.J., Rosen, M.J., Han, A.W., Johnson, A.J.A., Holmes, S.P., 2016. DADA2: High-resolution sample inference from Illumina amplicon data. Nature methods, 13:581-583.
9. Cantalapiedra, C.P., Hernández-Plaza, A., Letunic, I., Bork, P., Huerta-Cepas, J., 2021. eggNOG-mapper v2: functional annotation, orthology assignments, and domain prediction at the metagenomic scale. Molecular biology and evolution, 38:5825-5829.
10. Caporaso, J.G., Lauber, C.L., Walters, W.A., Berg-Lyons, D., Lozupone, C.A., Turnbaugh, P.J., Fierer, N., Knight, R., 2011. Global patterns of 16S rRNA diversity at a depth of millions of sequences per sample. Proceedings of the national academy of sciences, 108:4516-4522.
11. Carlson Jr, P.R., Forrest, J., 1982. Uptake of dissolved sulfide by Spartina alterniflora: evidence from natural sulfur isotope abundance ratios. Science, 216:633-635.
12. Chaumeil, P.A., Mussig, A.J., Hugenholtz, P., Parks, D.H., 2022. GTDB-Tk v2: memory friendly classification with the genome taxonomy database. Bioinformatics, 38:5315-5316.
13. Crump, B.C., Wojahn, J.M., Tomas, F., Mueller, R.S., 2018. Metatranscriptomics and amplicon sequencing reveal mutualisms in seagrass microbiomes. Frontiers in microbiology, 9:388.
14. David, A.S., Thapa-Magar, K.B., Menges, E.S., Searcy, C.A., Afkhami, M.E., 2020. Do plant–microbe interactions support the Stress Gradient Hypothesis?. Ecology, 101:e03081.
15. Dollhopf, S.L., Hyun, J.H., Smith, A.C., Adams, H.J., O'Brien, S., Kostka, J.E., 2005. Quantification of ammonia-oxidizing bacteria and factors controlling nitrification in salt marsh sediments. Applied and environmental microbiology, 71:240-246.
16. Donnelly, J.P., Bertness, M.D., 2001. Rapid shoreward encroachment of salt marsh cordgrass in response to accelerated sea-level rise. Proceedings of the National Academy of Sciences, 98:14218-14223.
17. Duarte, C.M., Losada, I.J., Hendriks, I.E., Mazarrasa, I., Marbà, N., 2013. The role of coastal plant communities for climate change mitigation and adaptation. Nature climate change, 3:961-968.
18. Farquhar, G.D., 1983. On the nature of carbon isotope discrimination in C4 species. Functional Plant Biology, 10:205-226.
19. Fox-Kemper, B., Hewitt, H.T., Xiao, C., Aðalgeirsdóttir, G., Drijfhout, S.S., et al. 2021. Ocean, cryosphere and sea level change. In Climate Change 2021: The Physical Science Basis. Contribution of Working Group I to the Sixth Assessment Report of the Intergovernmental Panel on Climate Change, ed. V Masson-Delmotte, P Zhai, A Pirani, SL Connors, C Péan, et al., pp. 1211–362. Cambridge, UK: Cambridge Univ. Press

20. Gandy, E.L., Yoch, D.C., 1988. relationship between nitrogen-fixing sulfate reducers and fermenters in salt marsh sediments and roots of *Spartina alterniflora*. Applied and Environmental Microbiology, 54:2031-2036.
21. García-Robledo, E., Corzo, A., Papaspyrou, S., 2014. A fast and direct spectrophotometric method for the sequential determination of nitrate and nitrite at low concentrations in small volumes. Marine Chemistry, 162:30-36.
22. Guimond, J.A., Yu, X., Seyfferth, A.L., Michael, H.A., 2020. Using hydrological-biogeochemical linkages to elucidate carbon dynamics in coastal marshes subject to relative sea level rise. Water Resources Research, 56:e2019WR026302.
23. Herbert, R.A., 1999. Nitrogen cycling in coastal marine ecosystems. FEMS microbiology reviews, 23:563-590.
24. Holmer, M., Gribsholt, B., Kristensen, E., 2002. Effects of sea level rise on growth of *Spartina anglica* and oxygen dynamics in rhizosphere and salt marsh sediments. Marine Ecology Progress Series, 225:197-204.
25. Howarth, R.W., 1984. The ecological significance of sulfur in the energy dynamics of salt marsh and coastal marine sediments. Biogeochemistry, 1:5-27.
26. Hwang, Y.H. and Morris, J.T., 1992. Fixation of inorganic carbon from different sources and its translocation in Spartina alterniflora Loisel. Aquatic botany, 43(2), pp.137-147.
27. Hyatt, D., Chen, G.L., LoCascio, P.F., Land, M.L., Larimer, F.W. and Hauser, L.J., 2010. Prodigal: prokaryotic gene recognition and translation initiation site identification. BMC bioinformatics, 11(1), p.119.
28. Johnston, E.R., Kim, M., Hatt, J.K., Phillips, J.R., Yao, Q., Song, Y., Hazen, T.C., Mayes, M.A., Konstantinidis, K.T., 2019. Phosphate addition increases tropical forest soil respiration primarily by deconstraining microbial population growth. Soil Biology and Biochemistry, 130:43-54.
29. Jørgensen, B.B., Findlay, A.J., Pellerin, A., 2019. The biogeochemical sulfur cycle of marine sediments. Frontiers in microbiology, 10:849.
30. Kang, D.D., Li, F., Kirton, E., Thomas, A., Egan, R., An, H. and Wang, Z., 2019. MetaBAT 2: an adaptive binning algorithm for robust and efficient genome reconstruction from metagenome assemblies. PeerJ, 7, p.e7359.
31. Kirwan, M.L., Temmerman, S., Skeehan, E.E., Guntenspergen, G.R., Fagherazzi, S., 2016. Overestimation of marsh vulnerability to sea level rise. Nature Climate Change, 6:253-260.
32. Kolton, M., Rolando, J.L. and Kostka, J.E., 2020. Elucidation of the rhizosphere microbiome linked to Spartina alterniflora phenotype in a salt marsh on Skidaway Island, Georgia, USA. FEMS Microbiology Ecology, 96(4), p.fiaa026.
33. Koop-Jakobsen, K., Mueller, P., Meier, R.J., Liebsch, G., Jensen, K., 2018. Plant-Sediment Interactions in Salt Marshes–An Optode Imaging Study of O_2, pH, and CO_2 Gradients in the Rhizosphere. Frontiers in plant science, 9:541.
34. Kopylova, E., Noé, L., Touzet, H., 2012. SortMeRNA: fast and accurate filtering of ribosomal RNAs in metatranscriptomic data. Bioinformatics, 28:3211-3217.
35. Kostka, J.E., Gribsholt, B., Petrie, E., Dalton, D., Skelton, H.,Kristensen, E., 2002. The rates and pathways of carbon oxidation in bioturbated saltmarsh sediments. Limnology and Oceanography, 47:230-240.

36. Kristensen, E., Alongi, D.M., 2006. Control by fiddler crabs (*Uca vocans*) and plant roots (*Avicennia marina*) on carbon, iron, and sulfur biogeochemistry in mangrove sediment. Limnology and Oceanography, 51:1557-1571.
37. Lamers, L.P., Govers, L.L., Janssen, I.C., Geurts, J.J., Van der Welle, M.E., Van Katwijk, M.M., Van der Heide, T., Roelofs, J.G., Smolders, A.J., 2013. Sulfide as a soil phytotoxin—a review. Frontiers in plant science, 4:268.
38. Langmead, B., Salzberg S., 2012. Fast gapped-read alignment with Bowtie 2. Nature Methods, 9:357-359.
39. Lee, R.W., Kraus, D.W., Doeller, J.E., 1999. Oxidation of sulfide by *Spartina alterniflora* roots. Limnology and Oceanography, 44:1155-1159.
40. Leppänen, S.M., Salemaa, M., Smolander, A., Mäkipää, R., Tiirola, M., 2013. Nitrogen fixation and methanotrophy in forest mosses along a N deposition gradient. Environmental and Experimental Botany, 90:62-69.
41. Lever, M.A., Torti, A., Eickenbusch, P., Michaud, A.B., Šantl-Temkiv, T., Jørgensen, B.B., 2015. A modular method for the extraction of DNA and RNA, and the separation of DNA pools from diverse environmental sample types. Frontiers in Microbiology 6:476.
42. Li, H., 2012. seqtk Toolkit for processing sequences in FASTA/Q formats. GitHub.
43. Li, H., Handsaker, B., Wysoker, A., Fennell, T., Ruan, J., Homer, N., Marth, G., Abecasis, G., Durbin, R., 2009. The sequence alignment/map format and SAMtools. Bioinformatics, 25:2078-2079.
44. Lim, S.J., Alexander, L., Engel, A.S., Paterson, A.T., Anderson, L.C., Campbell, B.J., 2019a. Extensive thioautotrophic gill endosymbiont diversity within a single *Ctena orbiculata* (Bivalvia: Lucinidae) population and implications for defining host-symbiont specificity and species recognition. MSystems, 4:e00280-19.
45. Lim, S.J., Davis, B.G., Gill, D.E., Walton, J., Nachman, E., Engel, A.S., Anderson, L.C., Campbell, B.J., 2019b. Taxonomic and functional heterogeneity of the gill microbiome in a symbiotic coastal mangrove lucinid species. The ISME journal, 13:902-920.
46. Lundberg, D.S., Yourstone, S., Mieczkowski, P., Jones, C.D., Dangl, J.L., 2013. Practical innovations for high-throughput amplicon sequencing. Nature methods, 10:999-1002.
47. Martin, M., 2011. Cutadapt removes adapter sequences from high-throughput sequencing reads. EMBnet. journal, 17:10-12.
48. Martin, B.C., Middleton, J.A., Fraser, M.W., Marshall, I.P., Scholz, V.V., Hausl, B. and Schmidt, H., 2020a. Cutting out the middle clam: lucinid endosymbiotic bacteria are also associated with seagrass roots worldwide. The ISME journal, 14:2901-2905.
49. Martin, B.C., Alarcon, M.S., Gleeson, D., Middleton, J.A., Fraser, M.W., Ryan, M.H., Holmer, M., Kendrick, G.A., Kilminster, K., 2020b. Root microbiomes as indicators of seagrass health. FEMS Microbiology Ecology, 96:fiz201.
50. McGlathery, K.J., Risgaard-Petersen, N., Christensen, P.B., 1998. Temporal and spatial variation in nitrogen fixation activity in the eelgrass *Zostera marina* rhizosphere. Marine Ecology Progress Series, 168:245-258.
51. McMurdie, P.J. and Holmes, S., 2013. phyloseq: an R package for reproducible interactive analysis and graphics of microbiome census data. PloS one, 8:e61217.
52. Mendelssohn, I.A. and Morris, J.T., 2000. Eco-physiological controls on the primary productivity of *Spartina alterniflora*. Concepts and Controversies in Tidal Marsh Ecology, pp.59-80.

53. Morris, J. T., Cahoon, D. R., Callaway, J. C., Craft, C., Neubauer, S. C., Weston, N. B., 2021. Marsh Equilibrium Theory: Implications for Responses to Rising Sea Level. In: FitzGerald, D. M. and Hughes, Z. J. (eds) Salt Marshes: Function, Dynamics, and Stresses. Cambridge: Cambridge University Press, pp. 157–177.
54. Müller, A.L., Kjeldsen, K.U., Rattei, T., Pester, M., Loy, A., 2015. Phylogenetic and environmental diversity of DsrAB-type dissimilatory (bi) sulfite reductases. The ISME journal, 9:1152-1165.
55. Nayfach, S., Pollard, K.S. 2015. Average genome size estimation improves comparative metagenomics and sheds light on the functional ecology of the human microbiome. Genome Biology, 16:51.
56. Nayfach, S., Shi, Z.J., Seshadri, R., Pollard, K.S. and Kyrpides, N.C., 2019. insights from uncultivated genomes of the global human gut microbiome. Nature, 568:505-510.
57. Nielsen, L.B., Finster, K., Welsh, D.T., Donelly, A., Herbert, R.A., De Wit, R., Lomstein, B.A., 2001. Sulphate reduction and nitrogen fixation rates associated with roots, rhizomes and sediments from *Zostera noltii* and *Spartina maritima* meadows. Environmental Microbiology, 3:63-71.
58. Oksanen, J., Blanchet, F.G., Friendly, M., Kindt, R., Legendre, P., McGlinn, D., Minchin, P.R., O'Hara, R.B., Simpson, G.L., Solymos, P., Stevens, M.H.H., Szoecs, E., Wagner, H., 2020. vegan: Community Ecology Package. R package version 2.5-7. https://CRAN.R-project.org/package=vegan
59. Osvatic, J.T., Wilkins, L.G., Leibrecht, L., Leray, M., Zauner, S., Polzin, J., Camacho, Y., Gros, O., van Gils, J.A., Eisen, J.A., Petersen, J.M., 2021. Global biogeography of chemosynthetic symbionts reveals both localized and globally distributed symbiont groups. Proceedings of the National Academy of Sciences, 118:e2104378118.
60. Osvatic, J.T., Yuen, B., Kunert, M., Wilkins, L., Hausmann, B., Girguis, P., Lundin, K., Taylor, J., Jospin, G., Petersen, J.M., 2023. Gene loss and symbiont switching during adaptation to the deep sea in a globally distributed symbiosis. The ISME Journal, 17:453-466.
61. Peng, Y., Leung, H.C., Yiu, S.M., Chin, F.Y., 2012. IDBA-UD: a de novo assembler for single-cell and metagenomic sequencing data with highly uneven depth. Bioinformatics, 28:1420-1428.
62. Petersen, J.M., Kemper, A., Gruber-Vodicka, H., Cardini, U., Van Der Geest, M., Kleiner, M., Bulgheresi, S., Mußmann, M., Herbold, C., Seah, B.K., Antony, C.P., 2017. Chemosynthetic symbionts of marine invertebrate animals are capable of nitrogen fixation. Nature microbiology, 2:16195.
63. Petersen, J.M., Yuen, B., 2021. The symbiotic "all-rounders": partnerships between marine animals and chemosynthetic nitrogen-fixing bacteria. Applied and Environmental Microbiology, 87:e02129-20.
64. Price, M.N., Dehal, P.S. and Arkin, A.P., 2010. FastTree 2–approximately maximum-likelihood trees for large alignments. PloS one, 5:e9490.
65. Quast, C., Pruesse, E., Yilmaz, P., Gerken, J., Schweer, T., Yarza, P., Peplies, J., Glöckner, F.O., 2012. The SILVA ribosomal RNA gene database project: improved data processing and web-based tools. Nucleic acids research, 41:D590-D596.
66. Quinlan, A.R., Hall, I.M., 2010. BEDTools: a flexible suite of utilities for comparing genomic features. Bioinformatics, 26:841-842.

885 67. Rodriguez-R, L.M., Konstantinidis, K.T., 2016. The enveomics collection: a toolbox for
886 specialized analyses of microbial genomes and metagenomes. PeerJ Prepr 4: e1900v1.
887 68. Rodriguez-R, L.M., Gunturu, S., Harvey, W.T., Rosselló-Mora, R., Tiedje, J.M., Cole,
888 J.R., Konstantinidis, K.T., 2018a. The Microbial Genomes Atlas (MiGA) webserver:
889 taxonomic and gene diversity analysis of Archaea and Bacteria at the whole genome level.
890 Nucleic acids research, 46:W282-W288.
891 69. Rodriguez-R, L. M., Gunturu, S., Tiedje, J. M., Cole, J. R., Konstantinidis, K. T., 2018b.
892 Nonpareil 3: fast estimation of metagenomic coverage and sequence diversity. MSystems,
893 3:e00039-18.
894 70. Rodriguez-R, L.M., Tsementzi, D., Luo, C., Konstantinidis, K.T., 2020. Iterative
895 subtractive binning of freshwater chronoseries metagenomes identifies over 400 novel
896 species and their ecologic preferences. Environmental Microbiology, 22:3394-3412.
897 71. Rolando, J.L., Kolton, M., Song, T., Kostka, J.E., 2022. The core root microbiome of
898 *Spartina alterniflora* is predominated by sulfur-oxidizing and sulfate-reducing bacteria in
899 Georgia salt marshes, USA. Microbiome, 10:37.
900 72. Salazar, G., Paoli, L., Alberti, A., Huerta-Cepas, J., Ruscheweyh, H.J., Cuenca, M., Field,
901 C.M., Coelho, L.P., Cruaud, C., Engelen, S., Gregory, A.C., 2019. Gene expression
902 changes and community turnover differentially shape the global ocean
903 metatranscriptome. Cell, 179:1068-1083.
904 73. Sieber, C.M., Probst, A.J., Sharrar, A., Thomas, B.C., Hess, M., Tringe, S.G., Banfield,
905 J.F., 2018. Recovery of genomes from metagenomes via a dereplication, aggregation and
906 scoring strategy. Nature microbiology, 3:836-843.
907 74. Sievers, F., Wilm, A., Dineen, D., Gibson, T.J., Karplus, K., Li, W., Lopez, R., McWilliam,
908 H., Remmert, M., Söding, J., Thompson, J.D., 2011. Fast, scalable generation of high-
909 quality protein multiple sequence alignments using Clustal Omega. Molecular systems
910 biology, 7:539.
911 75. Simmons, T., Caddell, D.F., Deng, S., Coleman-Derr, D., 2018. Exploring the root
912 microbiome: extracting bacterial community data from the soil, rhizosphere, and root
913 endosphere. Journal of visualized experiments: JoVE, 135.
914 76. Spivak, A.C., Reeve, J., 2015. Rapid cycling of recently fixed carbon in a *Spartina*
915 *alterniflora* system: a stable isotope tracer experiment. Biogeochemistry, 125:97-114.
916 77. Thomas, F., Giblin, A.E., Cardon, Z.G., Sievert, S.M., 2014. Rhizosphere heterogeneity
917 shapes abundance and activity of sulfur-oxidizing bacteria in vegetated salt marsh
918 sediments. Frontiers in microbiology, 5:309.
919 78. Trivedi, P., Leach, J.E., Tringe, S.G., Sa, T., Singh, B.K., 2020. Plant–microbiome
920 interactions: from community assembly to plant health. Nature reviews microbiology,
921 18:607-621.
922 79. Wang, Q., Garrity, G.M., Tiedje, J.M., Cole, J.R., 2007. Naive Bayesian classifier for rapid
923 assignment of rRNA sequences into the bacterial taxonomy. Applied and environmental
924 microbiology, 73:5261-5267.
925 80. Welsh, D.T., Bourgues, S., de Wit, R., Herbert, R.A., 1996. Seasonal variations in nitrogen-
926 fixation (acetylene reduction) and sulphate-reduction rates in the rhizosphere of *Zostera*
927 *noltii*: nitrogen fixation by sulphate-reducing bacteria. Marine Biology, 125:619-628.
928 81. Whiting, G.J., Gandy, E.L., Yoch, D.C., 1986. Tight coupling of root-associated nitrogen
929 fixation and plant photosynthesis in the salt marsh grass *Spartina alterniflora* and carbon

930 dioxide enhancement of nitrogenase activity. Applied and environmental microbiology,
931 52:108-113.
932 82. Wu, Y.W., Simmons, B.A., Singer, S.W., 2016. MaxBin 2.0: an automated binning
933 algorithm to recover genomes from multiple metagenomic datasets. Bioinformatics,
934 32:605-607.
935 83. Yu, G., Lam, T.T.Y., Zhu, H., Guan, Y., 2018. Two methods for mapping and visualizing
936 associated data on phylogeny using ggtree. Molecular biology and evolution, 35:3041-
937 3043.

938
939
940
941
942
943
944
945
946
947
948
949
950
951
952
953
954
955
956
957
958
959
960
961

Figure 1. *Spartina alterniflora* biomass gradient as a natural laboratory. A gradient in *S. alterniflora* aboveground biomass is commonly observed with tall plants growing at the levees next to large tidal creeks and a short phenotype of *S. alterniflora* dominating the interior of the marsh. Sediments from the tall *S. alterniflora* zone are characterized as a more oxidized environment with higher levels of iron, coupled nitrification-denitrification as well as higher rates of organic matter hydrolysis and mineralization. Conversely, sediments from the short phenotype tend to be more chemically reduced, with higher rates of sulfate reduction, elevated porewater salinity, and less bioturbation and tidal flushing. Roots from the short *S. alterniflora* phenotype have been proposed to harbor sulfur-oxidizing bacteria (SOB) that benefit the plant by detoxifying the root environment.

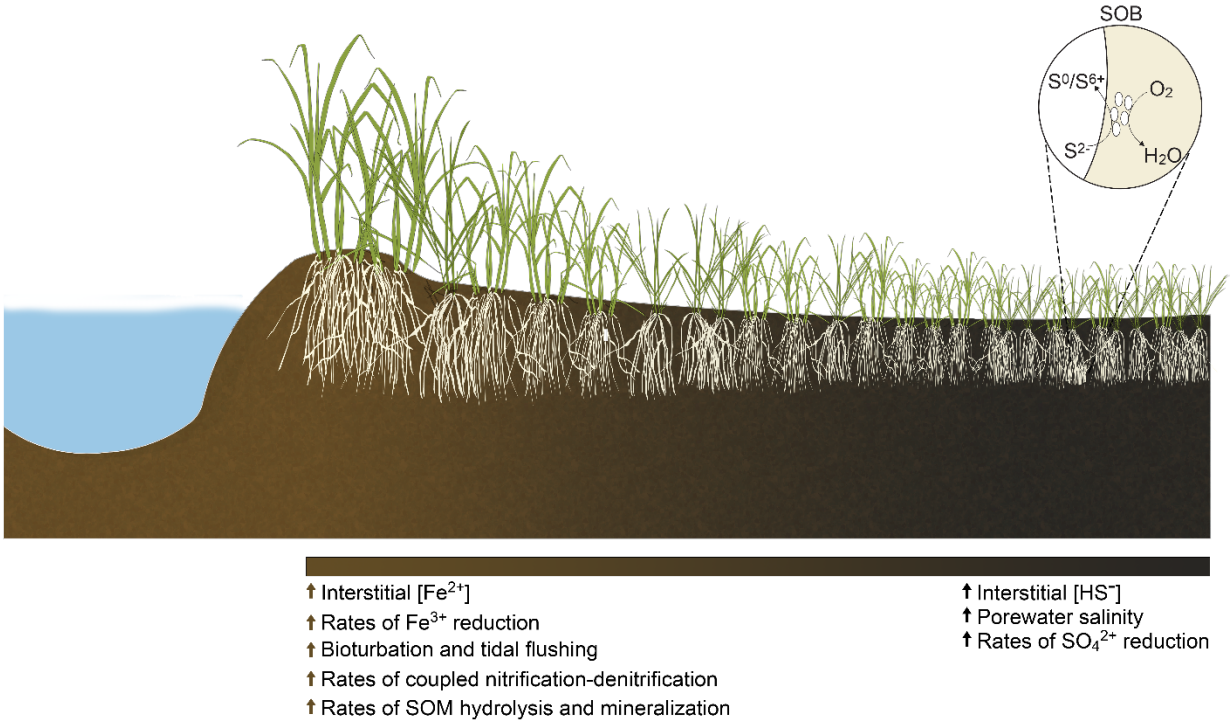

Figure 2. Phylogenetic reconstruction of 160 dereplicated high-quality metagenome assembled genomes (MAGs, > 50 quality-score) binned from *Spartina alterniflora* sediment, rhizosphere, and root samples. Outer rim shows the presence/absence of genes for carbon fixation (RuBisCO), nitrogen fixation (nifKDH), thiosulfate oxidation (soxABXYZ), dissimilatory sulfite reduction/oxidation (dsrAB), nitrification (amoCAB), denitrification, and dissimilatory nitrate reduction to ammonium (DNRA).

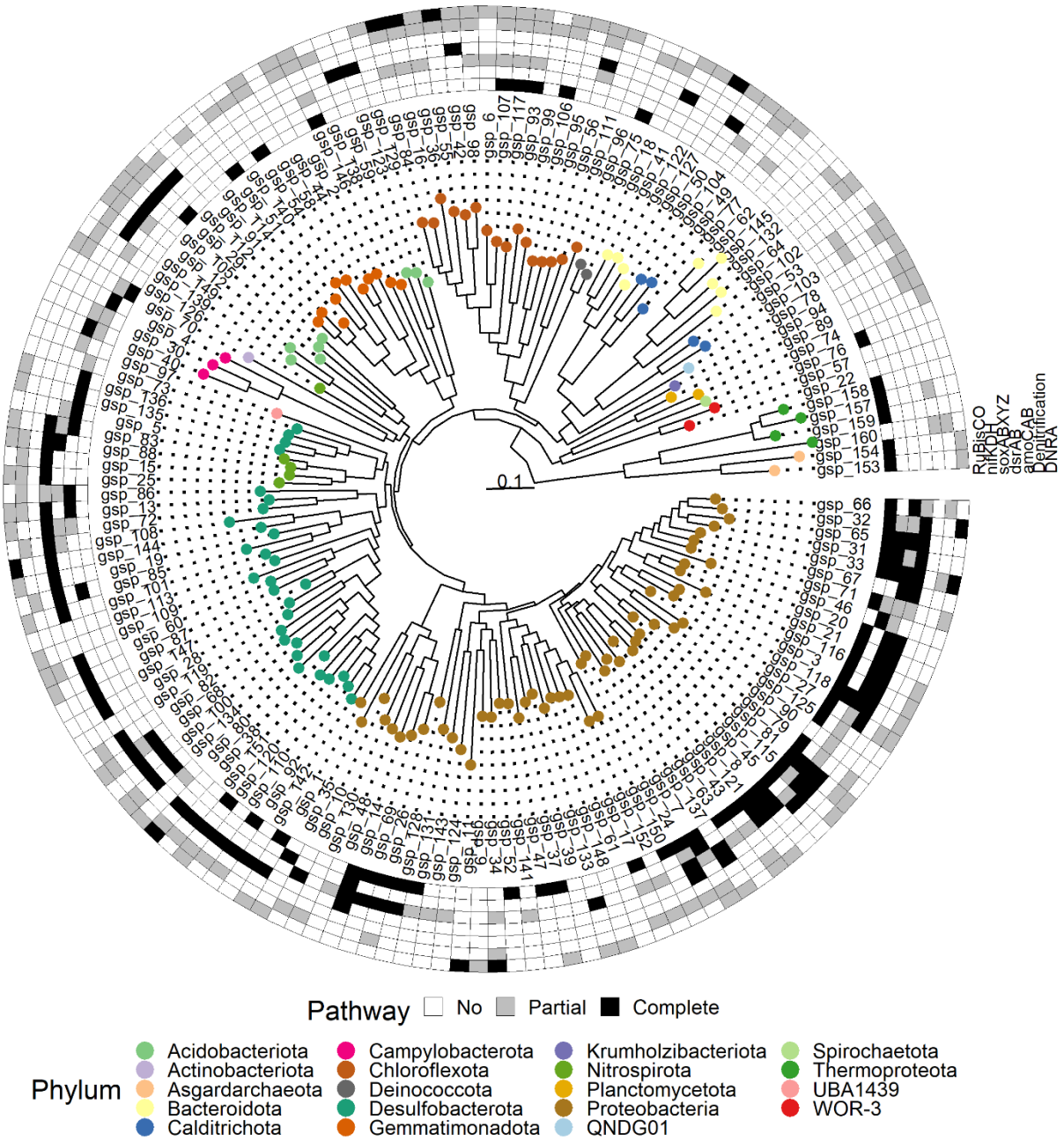

Figure 3. Drivers and metagenome assembled genomes (MAGs) associated with rates of N fixation and nitrification in the salt marsh environment. Rates of nitrification and N fixation (under anoxic and oxic conditions) per microbiome compartment and *Spartina alterniflora* phenotype (a). Normalized transcript relative abundance of the nitrogenase gene (nifK), and the reductive and oxidative dsrA types per microbiome compartment and *Spartina alterniflora* phenotype (b). Percentage from the total nitrogenase (nifK) and reductive and oxidative types of the dsrA transcripts mapping to the most active MAGs (c). Statistical significance based on non-parametric pairwise Mann-Whitney tests. n.s = p-value > 0.5, * p-value < 0.5, ** p-value < 0.01.

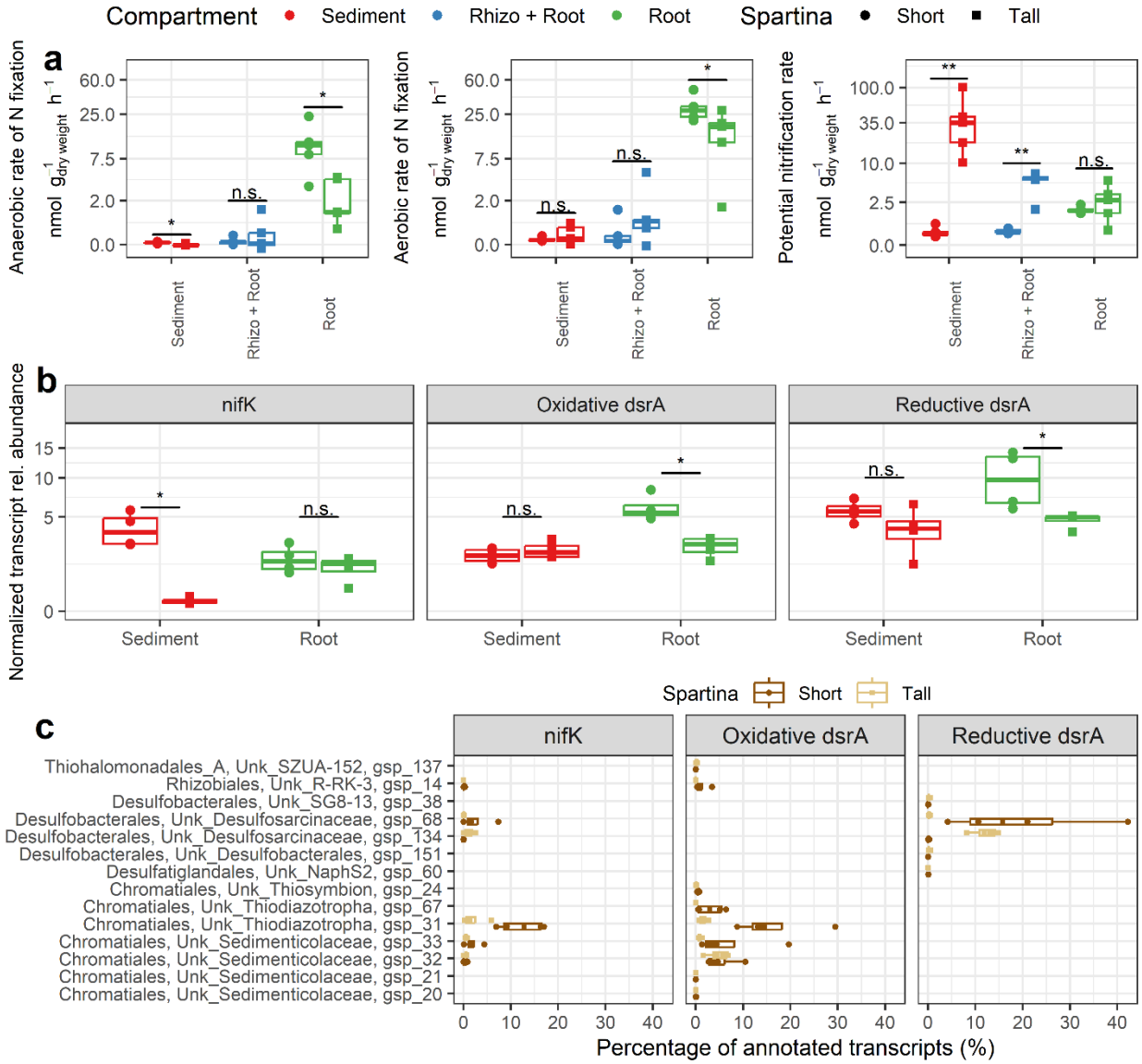

Figure 4. Phylogenetic tree of the Sedimenticolaceae family. Taxonomic annotation of the *Candidatus* Thiodiazotropha genus was based on Osvatic et al. (2023). The diagram next to the species name recognizes genomes recovered as symbionts of eukaryotic organisms. The average relative abundance of the metagenome assembled genomes (MAGs) from the present study is shown in the adjacent panels per microbiome compartment and *Spartina alterniflora* phenotype. Relative abundance was calculated at the DNA-level based on average coverage per position in metagenomic libraries. Purple sulfur bacteria *Allochromatium vinosum* was used as an outgroup for the phylogenetic tree.

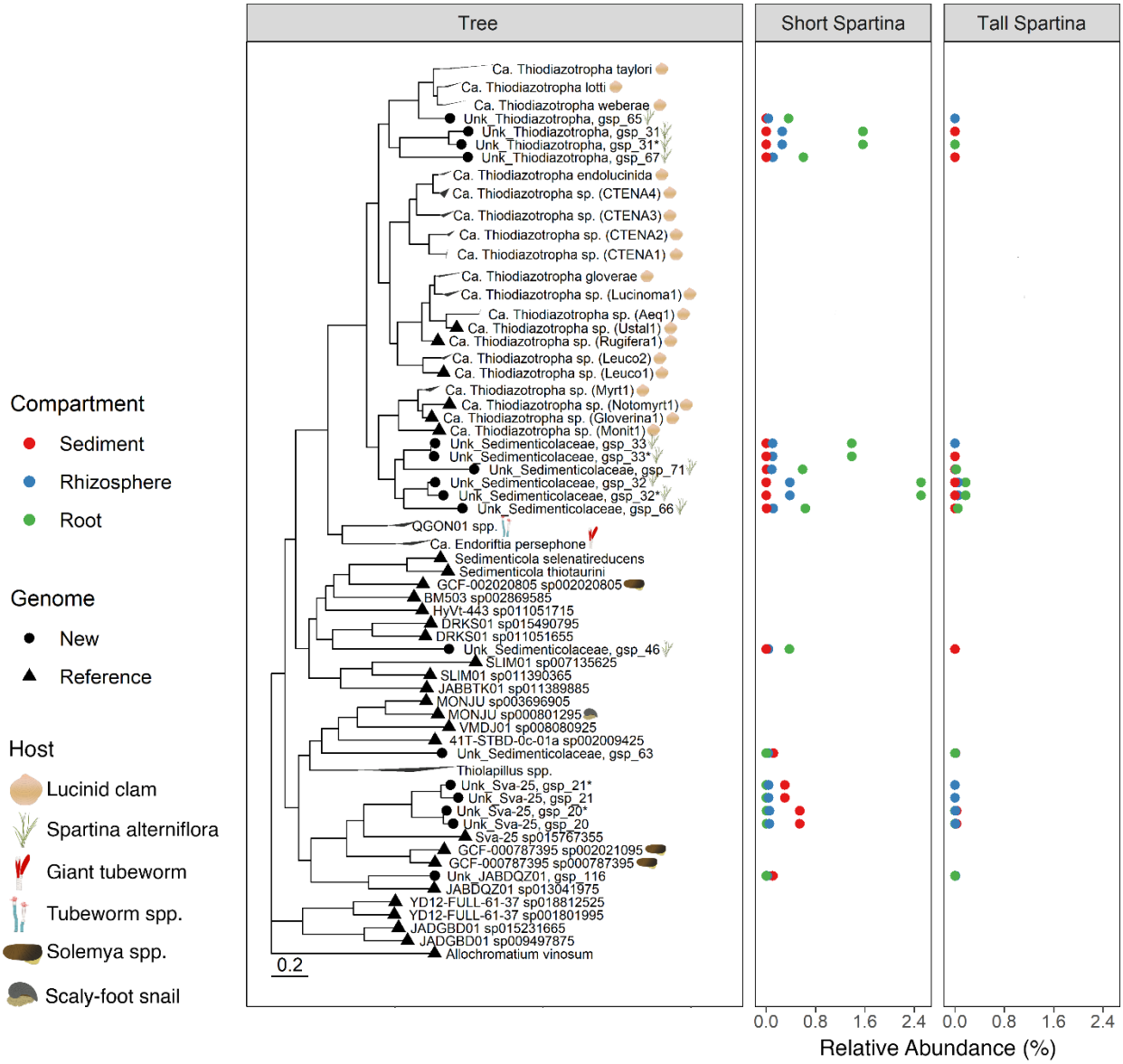

Figure 5. Prokaryotic abundance, functional diversity, and activity are determined by *Spartina alterniflora* phenotype and microbiome compartment. Average ± standard error of the metagenomic nonpareil diversity, 16S rRNA gene and transcript abundance as quantified by qPCR and RT-qPCR, respectively (n = 4) (a). Principal coordinate analysis (PCoA) ordination plot based on the Bray-Curtis dissimilatory index of functional profiles from KEGG orthology annotations (KO level) of metagenome and metatranscriptome libraries (b). Gene and transcript normalized relative abundance of prokaryotic terminal oxidases and selected enzymes of the carbon, nitrogen, and sulfur cycles (c). Different letter indicate statistical difference based on pairwise Mann-Whitney tests (p-value < 0.5).

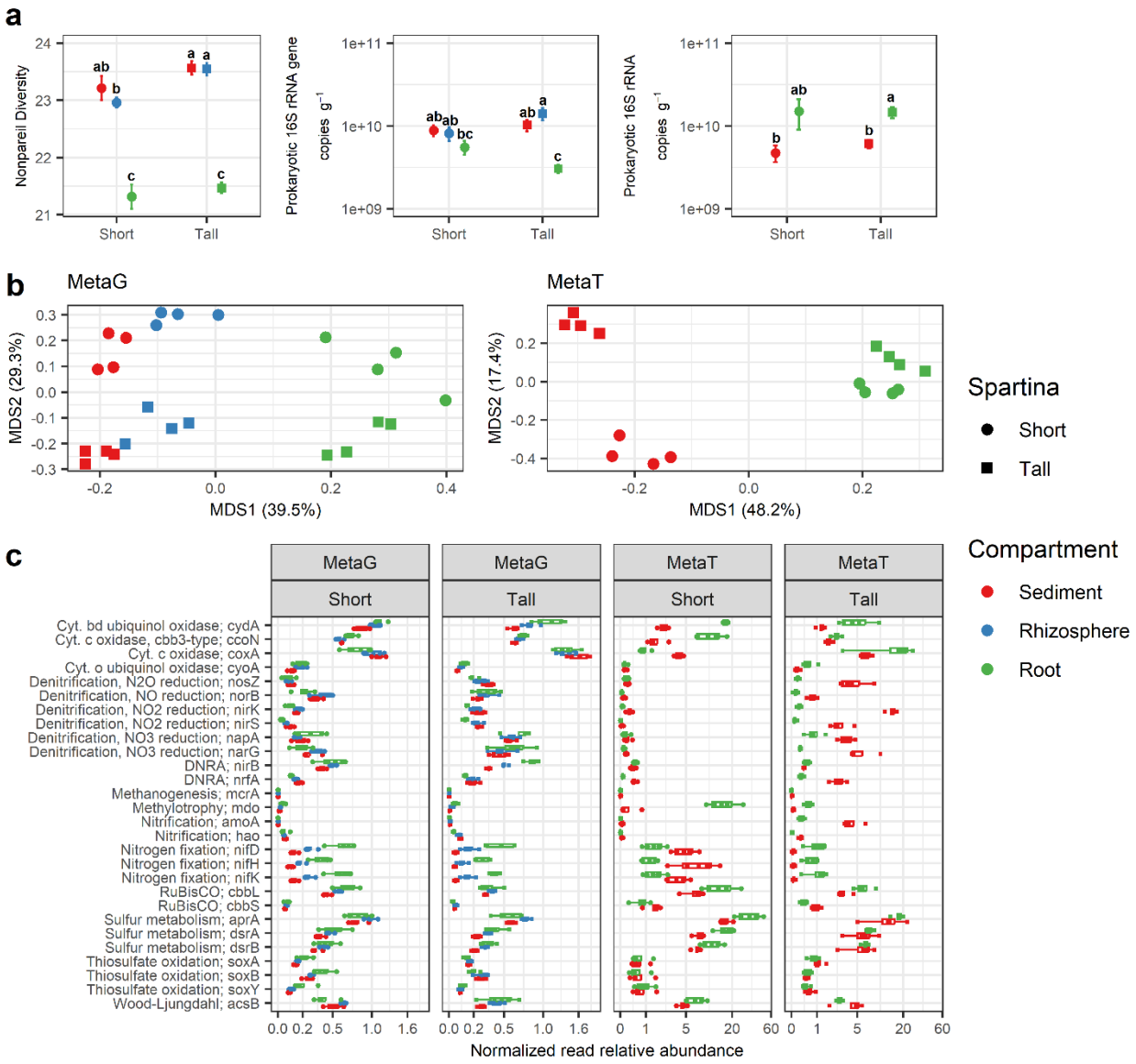

1026 **Figure 6:** Roots from marine influenced ecosystems assemble a distinct microbial community
1027 enriched by bacteria with known to conserve energy from sulfur metabolism. Non-metric
1028 multidimensional scaling (NMDS) ordination plot based on the Bray-Curtis dissimilatory index
1029 of root-associated prokaryotic communities at the genus level, colored by ecosystem type (a).
1030 Relative abundance of putative sulfur-oxidizing (b) and sulfate-reducing root bacteria (c) by
1031 ecosystem type. Prokaryotic communities were characterized by analyzing an SSU rRNA gene
1032 amplicon dataset of 1182 samples assessing roots from 56 plant species. Different letter indicate
1033 statistical difference based on pairwise Mann-Whitney tests (p-value < 0.5).

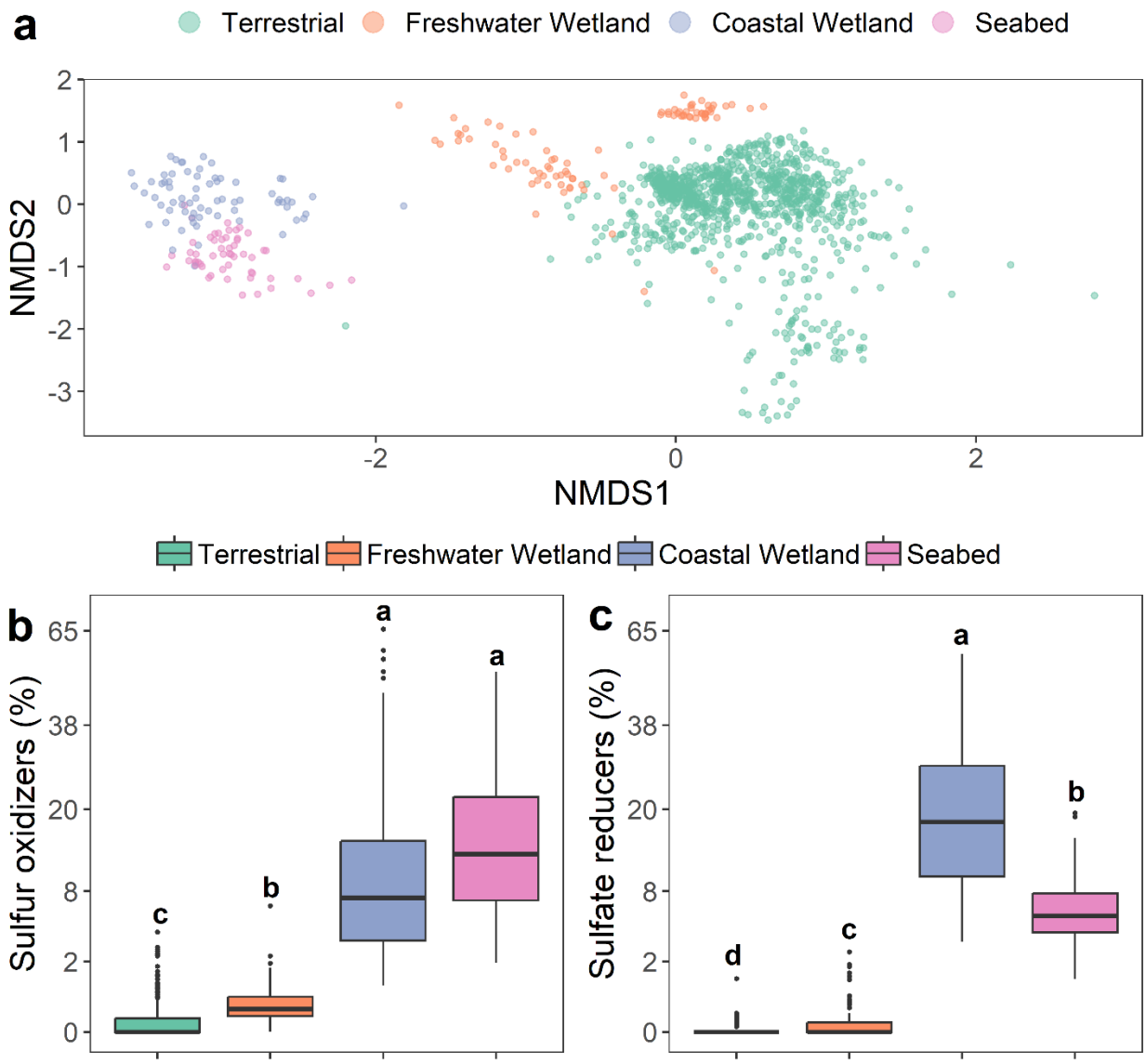

1034

1035

1036

1037

1038 **Supplementary Figure S1.** dsrAB phylogenetic tree of genes retrieved from metagenome-
1039 assembled genomes (MAGs). Genes were aligned to a reference database and tree was
1040 constructed with FastTree v.2.1.11. Oxidative and reductive types of the dsrAB gene were
1041 inferred based on phylogenetic placement in the constructed tree. Archean *Pyrobaculum*
1042 *aerophilum* was used as an outgroup.

1043

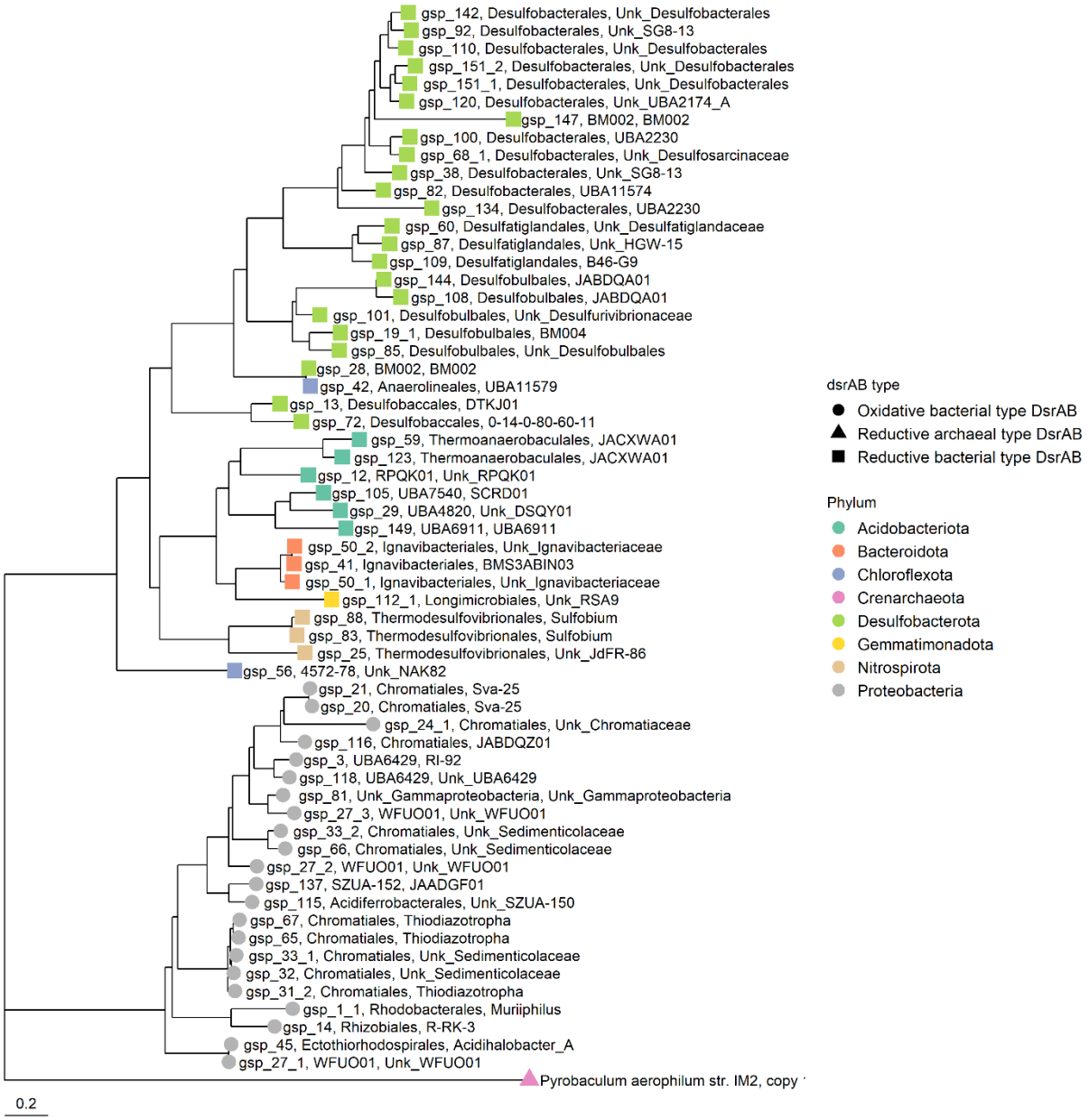

1044

1045

1046

1047

Supplementary Figure S2. Phylogenetic tree of the oxidative dsrAB type from metagenome assembled genomes (MAGs) aligned to a reference alignment database (Müller et al., 2015). Archean *Pyrobaculum aerophilum* was used as an outgroup of the phylogenetic tree.

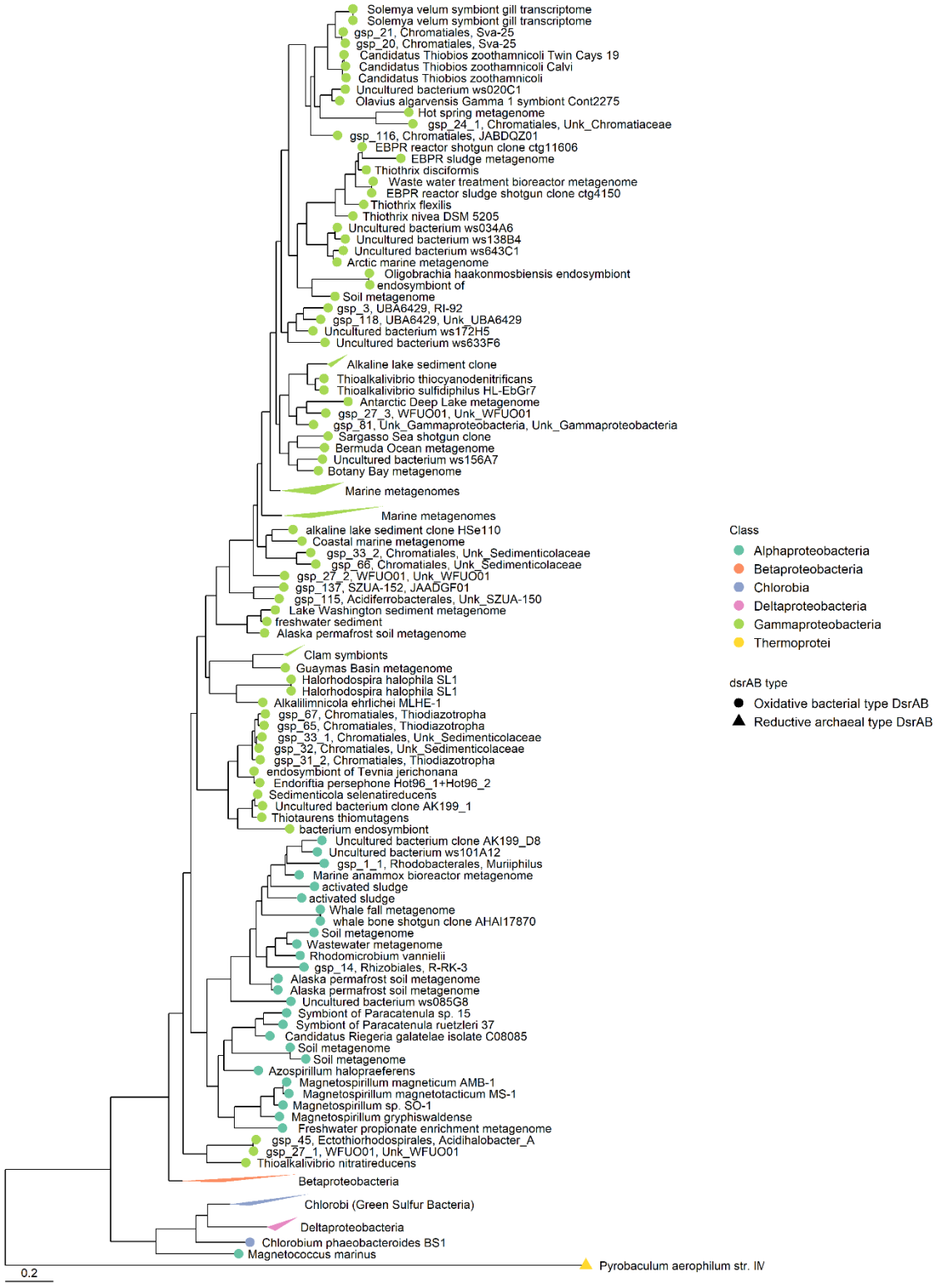

Supplementary Figure S3. Gene expression of the nitrogenase (nifD, nifK, and nifH) and dissimilatory sulfite reductase genes (dsrA, dsrB, and aprA) are highly correlated among their own metabolic pathways.

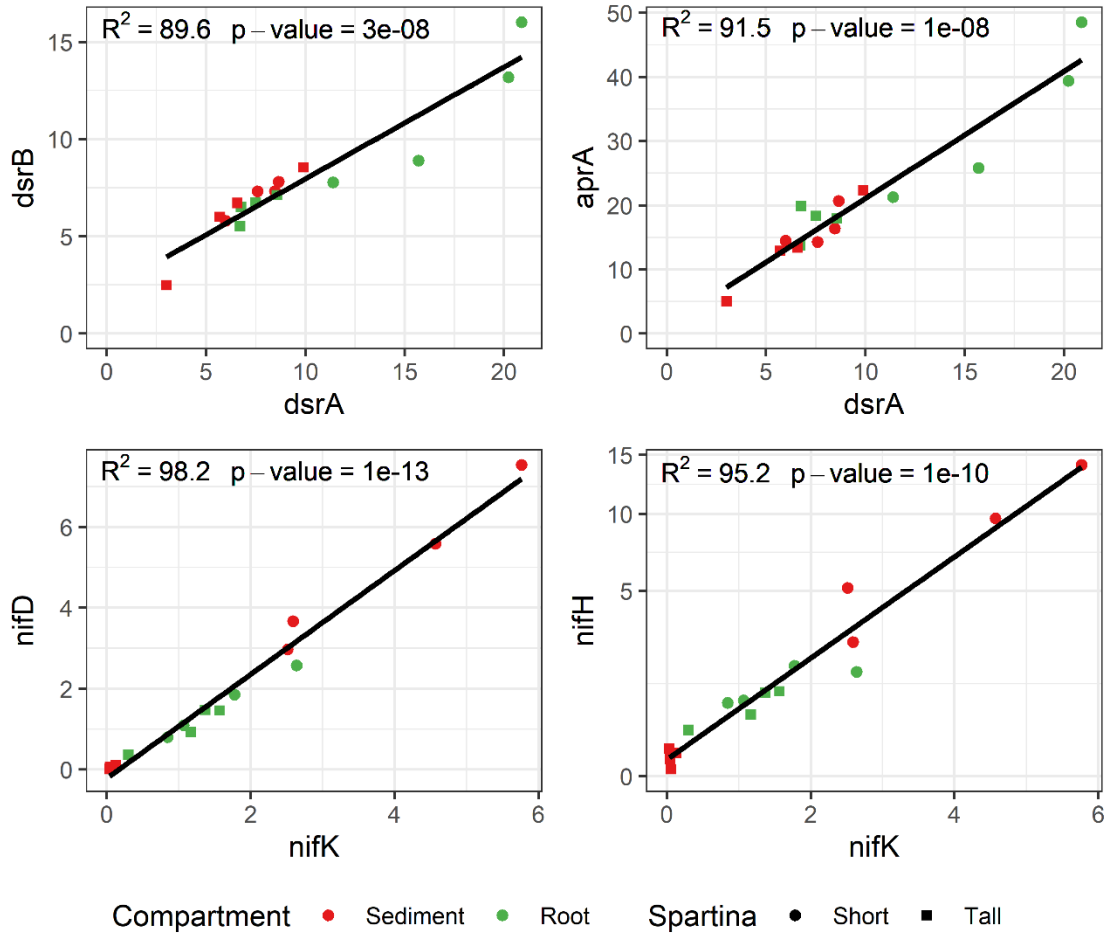

1065 **Supplementary Figure S4.** Relation between the gene expression of the *Ca.* Thiodiazotropha
1066 sp. (gsp 31) oxidative, and *Desulfosarcinaceae* sp. (gsp. 68) reductive dsrA gene and the
1067 nitrogenase gene nifK in *Spartina alterniflora* root samples. Gene expression measured as the
1068 percentage of transcripts mapping to each genomospecies from the totality of functionally
1069 annotated short read transcripts.

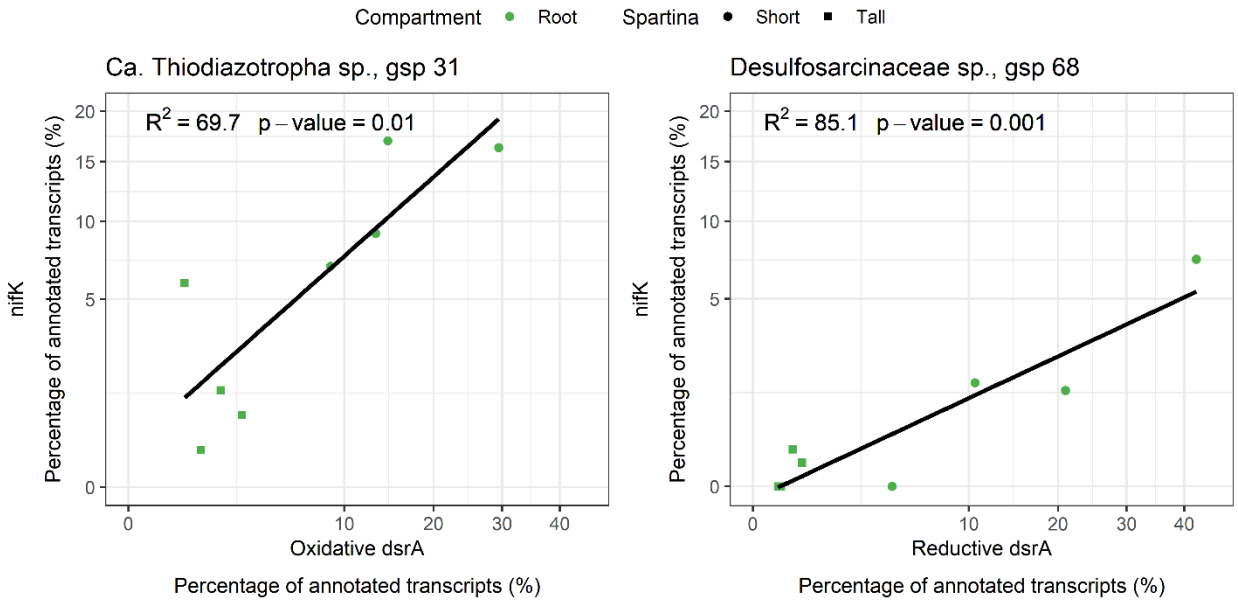

1070
1071
1072
1073
1074
1075
1076
1077
1078
1079
1080
1081
1082
1083
1084

1085 **Supplementary Figure S5**. Gene and transcript relative abundance of the nitrogenase gene
1086 (nifK) partitioned at the finest taxonomic level as predicted by eggnog-mapper per microbiome
1087 compartment and *Spartina alterniflora* phenotype.

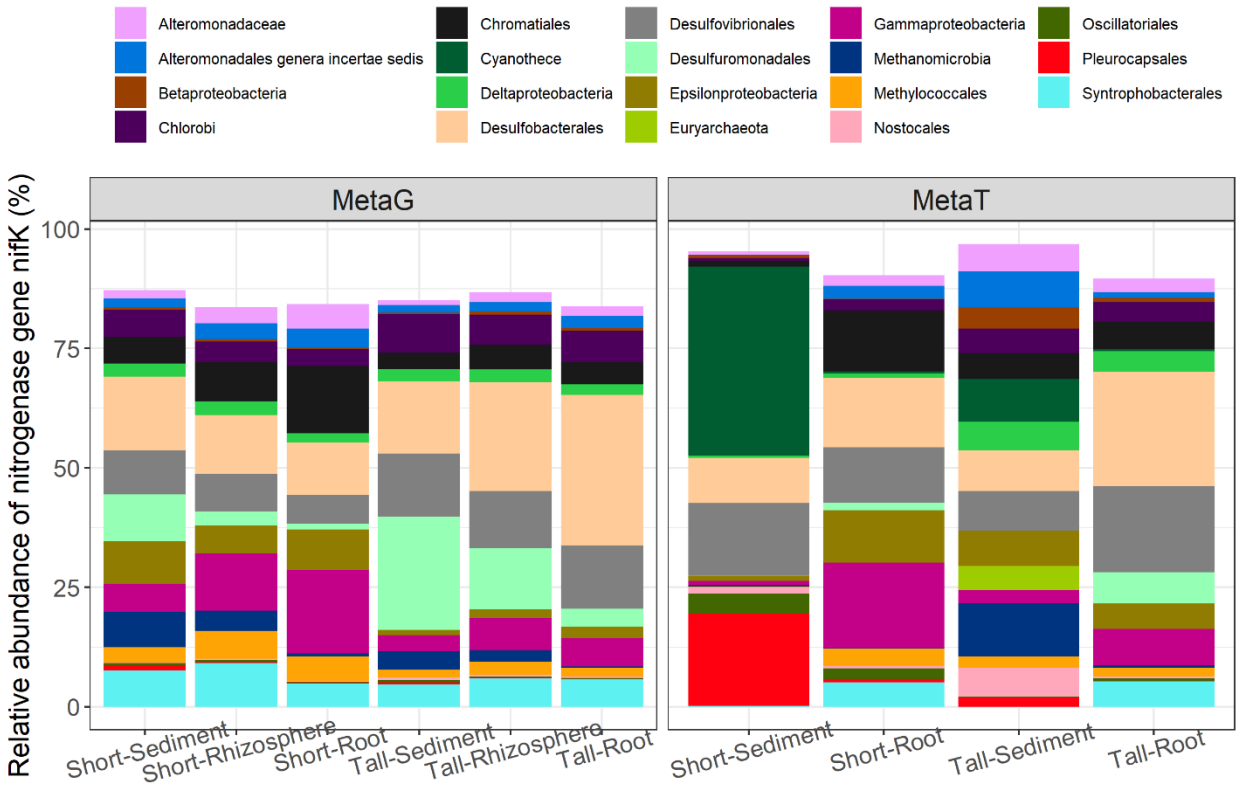

1088
1089
1090
1091
1092
1093
1094
1095
1096
1097
1098
1099
1100

1101 **Supplementary Figure S6.** Gene and transcript relative abundance of the oxidative dsrA gene
1102 partitioned at the finest taxonomic level as predicted by eggnog-mapper per microbiome
1103 compartment and *Spartina alterniflora* phenotype.

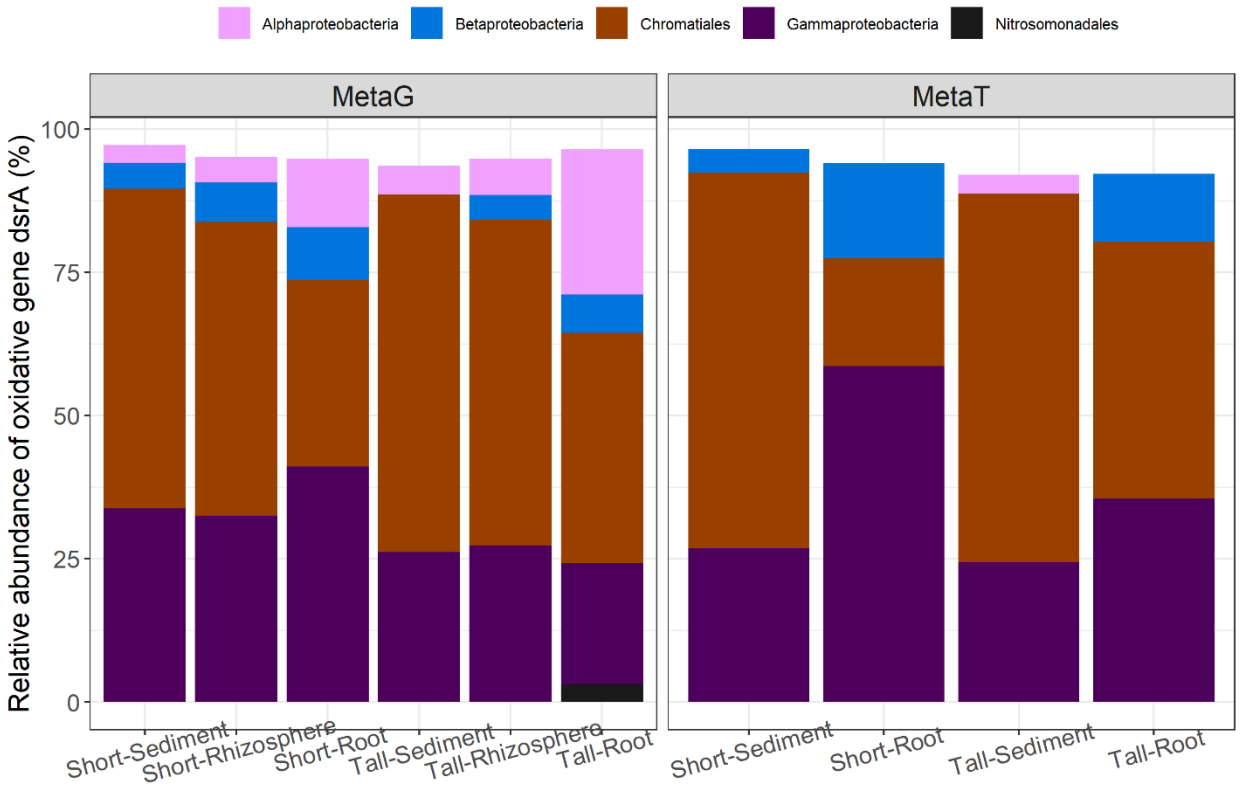

1104
1105
1106
1107
1108
1109
1110
1111
1112
1113
1114
1115
1116

1117 **Supplementary Figure S7.** Gene and transcript relative abundance of the reductive dsrA gene
1118 partitioned at the finest taxonomic level as predicted by eggnog-mapper per microbiome
1119 compartment and *Spartina alterniflora* phenotype.

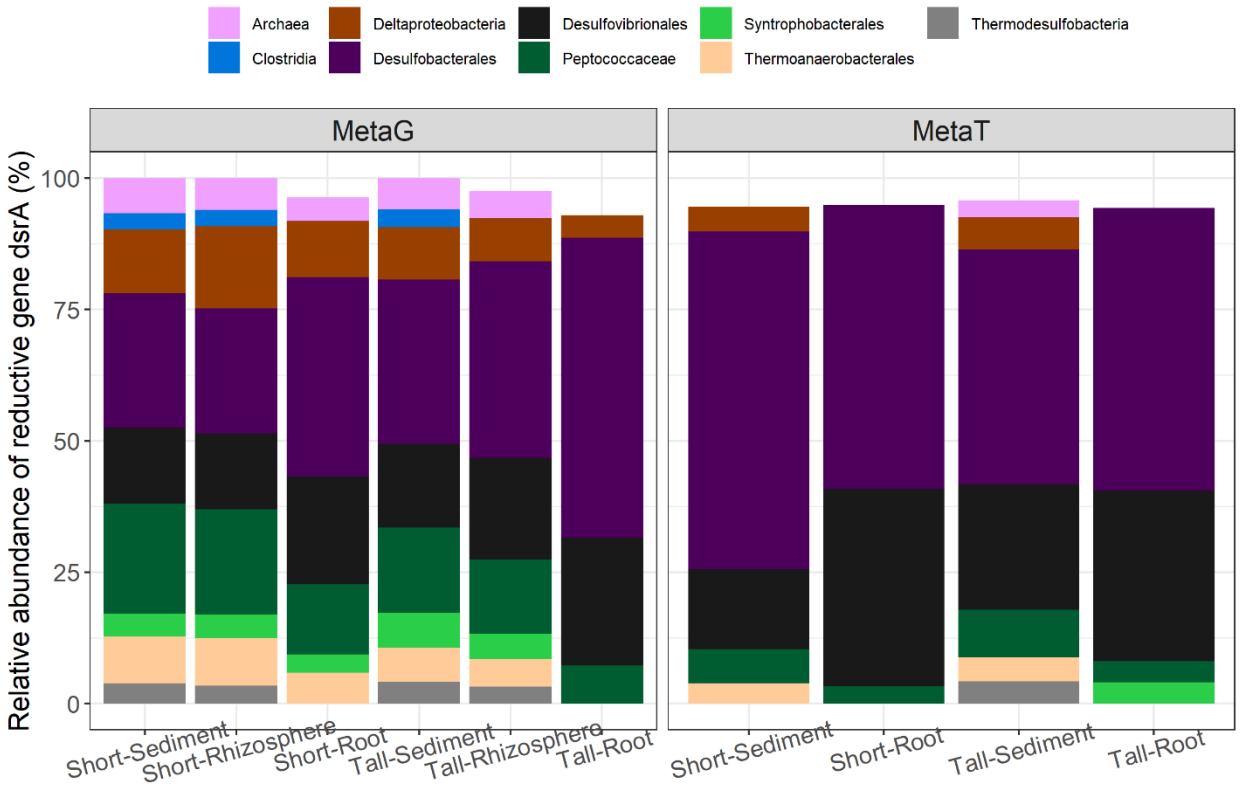

1120
1121
1122
1123
1124
1125
1126
1127
1128
1129
1130
1131
1132

Supplementary Figure S8. Relative abundance of selected metagenome assembled genomes (MAGs) from the *Desulfosarcinaceae* family across *Spartina alterniflora* phenotype and sampled compartment. Relative abundance was calculated at the DNA-level based on average coverage per position in metagenomic libraries. Different letter indicate statistical difference based on pairwise Mann-Whitney tests (p-value < 0.5).

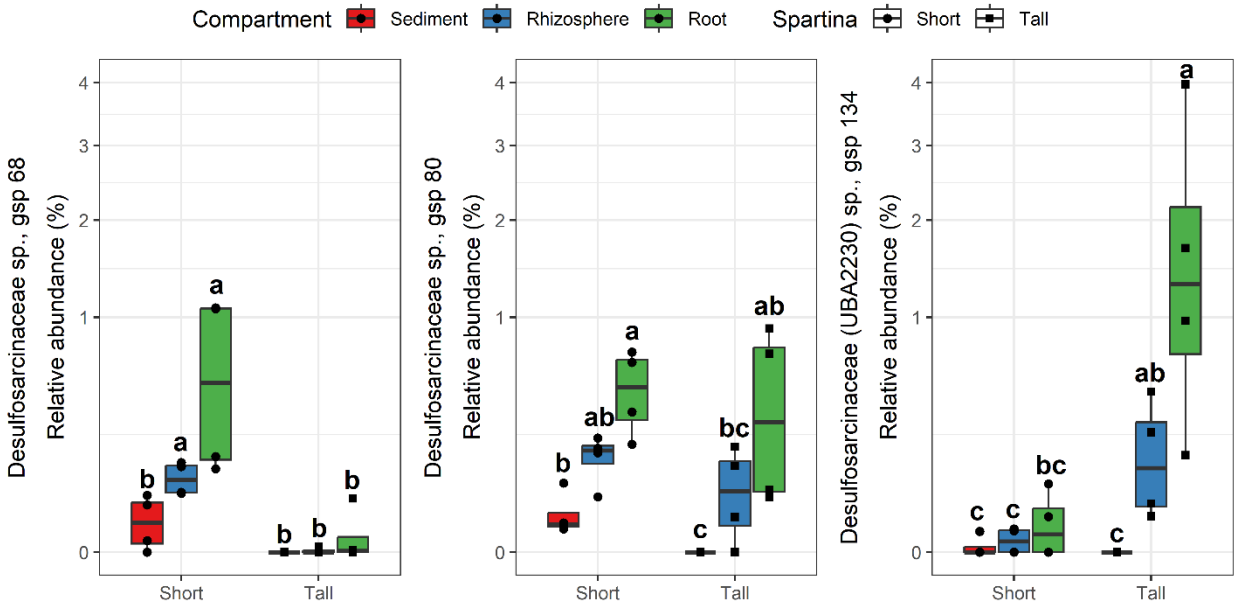

Supplementary Figure S9. Relative abundance of amplicon sequence variants (ASVs) classified as members of the *Desulfosarcinaceae* and *Sedimenticolaceae* families, and the *Desulfatitalea* and *Ca.* Thiodiazotropha genera across soil/sediment, rhizosphere, and root samples from a seabed, coastal wetland, freshwater wetland and terrestrial ecosystems dataset.

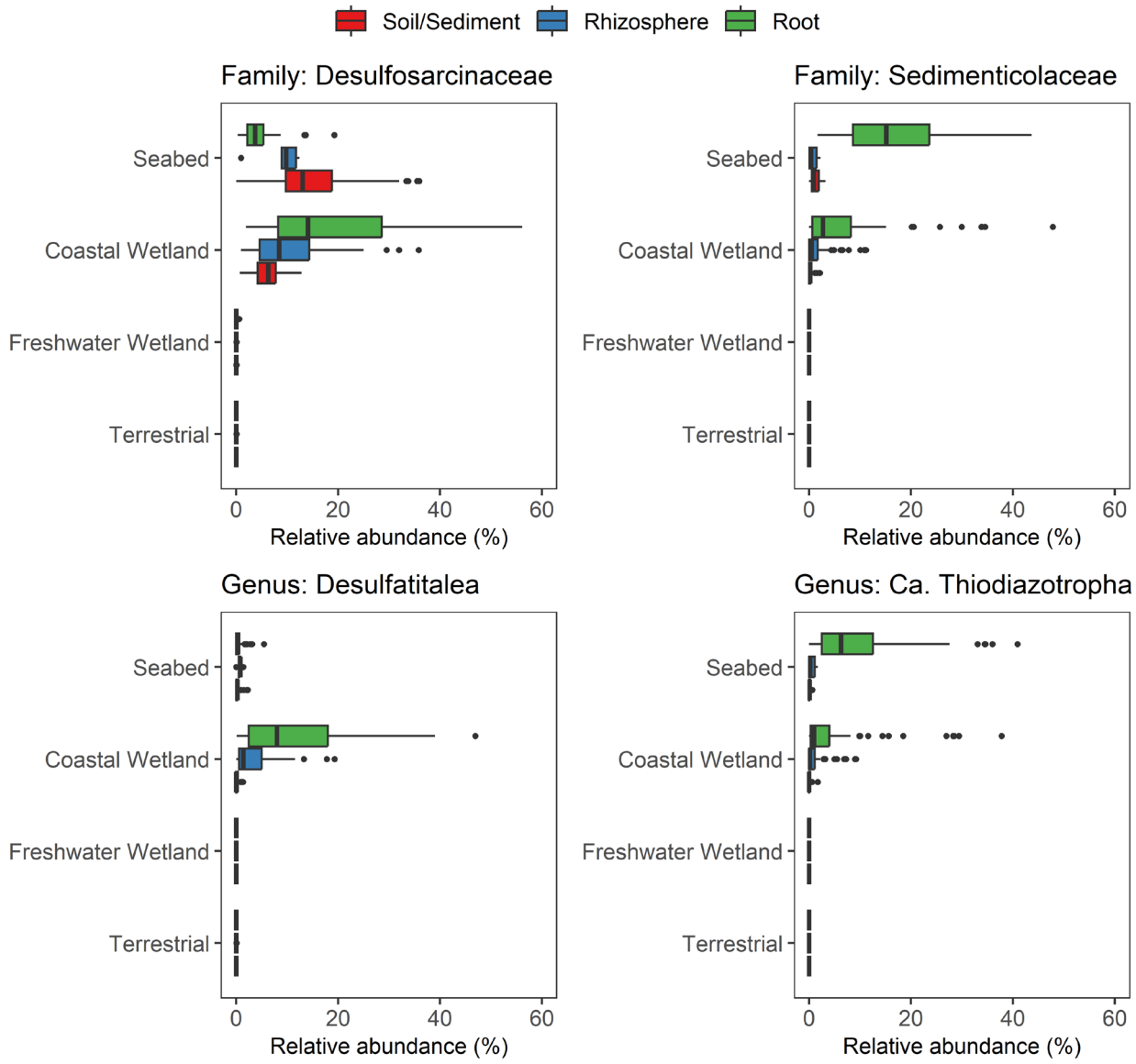

1163 **Supplementary Figure S10.** Root carbon ^{13}C isotopic natural abundance by *Spartina*
1164 *alterniflora* phenotype. ^{13}C natural abundance was expressed as the per mille (‰) deviation from
1165 the Pee Dee Belemnite standard (PDB) ^{13}C:^{12}C ratio ($\delta^{13}C$).

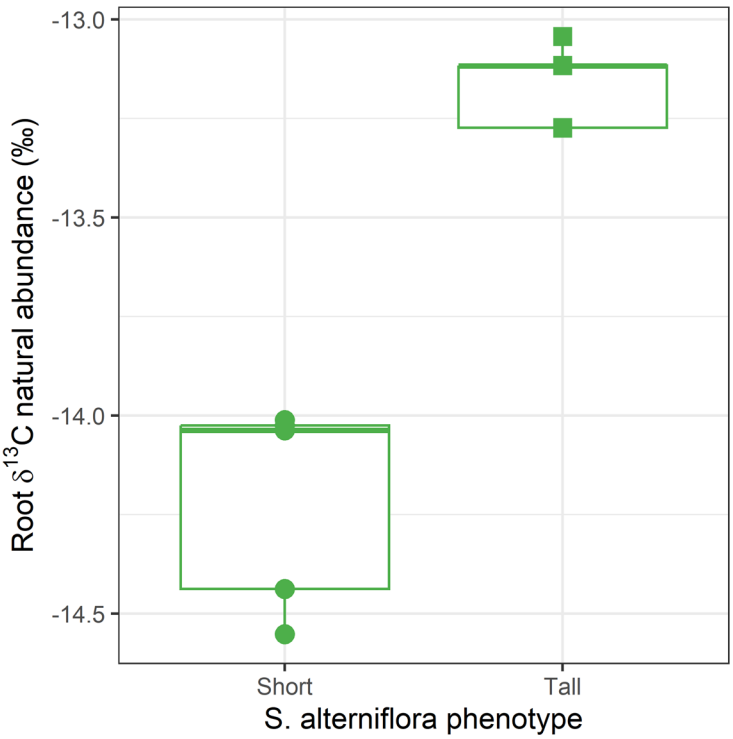

1166

1167

1168

1169